

DEPARTMENT OF PHYSICS
UNIVERSITY OF JYVÄSKYLÄ
RESEARCH REPORT NO. 9/2015

**UNCERTAINTY ANALYSIS AND SYMMETRY
RESTORATION IN NUCLEAR SELF-CONSISTENT
METHODS**

by

Yuan Gao

Supervisor: Professor Jacek Dobaczewski

Academic Dissertation
for the Degree of
Doctor of Philosophy

*To be presented, by permission of the
Faculty of Mathematics and Science
of the University of Jyväskylä,
for public examination in Auditorium YAA303 of the
University of Jyväskylä on December 16, 2015
at 12 o'clock noon*



JYVÄSKYLÄN YLIOPISTO

Jyväskylä, Finland

December 2015

Preface

The work presented in this thesis was carried out at the Department of Physics of the University of Jyväskylä during the year 2012-2015, within the Finland Distinguished Professor Programme (FIDIPRO).

First of all, I would like to thank my supervisor, Prof. Jacek Dobaczewski for his excellent guidance, insightful advice, and endless patience. I want to express my gratitude to all members of the FIDIPRO for all the fruitful discussions, especially Markus Kortelainen, Karim Ben-naceur, Jussi Toivanen, Andrea Idini, Tomohiro Oishi, Gianluca Salvioni, Yue Shi, and Lingfei Yu. I would like to thank the staff members of the Department of Physics of the University of Jyväskylä for their help. I also want to thank Prof. Luis Robledo and Dr. Nicolas Schunck for reviewing the manuscript and Prof. Wojciech Satula for promising to be my opponent.

Finally, I wish to thank my family and friends for their support.

Jyväskylä, Winter 2015

Yuan Gao

Abstract

This thesis contains two articles, in the following denoted by I and II, and an introduction to them. In Chapter 1, I present the theoretical models of nuclear structure. In Chapter 2, I introduce the basic ideas about the density functional theory (DFT) and self-consistent mean-field (SCMF) calculations. In Chapter 3, I give the formulae for the uncertainty propagation, which is the error analysis method used in article I. As a proper tool to survey the predictive power of theoretical models, the error analysis now has become more and more widely used. By analyzing the propagation of uncertainties, one tries to find out the effectiveness of the calculation with a given parameter set obtained from optimization. In Chapter 4, I present the theoretical framework of the Lipkin method used in article II. This method can be considered as an approximation of the variation-after-projection method. In Chapter 6, I briefly review the main results of articles I and II. In the Appendices, I give some useful details and derivations.

Author	Yuan Gao Department of Physics University of Jyväskylä Finland
Supervisor	Prof. Jacek Dobaczewski Department of Physics, University of Jyväskylä, Finland Department of Physics, University of York, United Kingdom Helsinki Institute of Physics, Finland
Reviewer	Prof. Luis Robledo Departamento de Física Teórica, Facultad de Ciencias, Universidad Autónoma de Madrid, Spain Dr. Nicolas Schunck Lawrence Livermore National Laboratory, USA
Opponent	Prof. Wojciech Satula Institute of Theoretical Physics, Faculty of Physics, University of Warsaw, Poland

List of Publications

I Propagation of uncertainties in the Skyrme energy-density-functional model

Y. Gao, J. Dobaczewski, M. Kortelainen, J. Toivanen and D. Tarpanov
Phys. Rev. C 87, 034324 (2013)

II Approximate restoration of translational and rotational symmetries within the Lipkin method

Y. Gao, J. Dobaczewski and P. Toivanen
arXiv:1511.02814

Both articles focus on how to improve the results of self-consistent mean-field calculations. In article I, the author has implemented the necessary numerical infrastructure based on the code HOSPHE [1] to determine uncertainties of the calculated observables, performed all numerical calculations of uncertainties, and participated in writing article I.

In article II, the author has derived the general formula for calculating average values of a given type of the Lipkin operators. He extended, debugged, and tested the part of the code HFODD [2] used for the Lipkin-method translational-symmetry restoration without pairing and fully implemented calculations with pairing interaction included. The author also implemented the entire numerical infrastructure needed for performing the Lipkin-method calculations for the rotational-symmetry restoration. Then, the author performed all numerical calculations and prepared a draft of the publication.

Contents

1	Introduction	11
2	DFT and MF	13
2.1	General concepts of DFT	13
2.2	SCMF method in nuclear system	16
2.2.1	The EDF from the Hartree-Fock average	16
2.2.2	SCMF equation	17
2.2.3	The EDF Generator	18
2.2.4	S-SC-MF-EDF calculation	19
2.3	Possible improvements	20
2.3.1	Improving the EDF generator	20
2.3.2	Generalizing the state	21
3	Propagation of uncertainties	27
3.1	The equations of propagation of uncertainties	27
3.2	Transformation between parameter sets	29
4	The Lipkin method	31
4.1	General concepts of the Lipkin method	31
4.2	Determination of $f(\hat{O})$	32
4.2.1	The Taylor expansion	32
4.2.2	The expression for \mathcal{A}	34
4.2.3	Transition density	34
4.2.4	The Gaussian overlap approximation	36
4.3	The LM for the T & R symmetry restoration	37
4.3.1	\hat{O} , \hat{Q} and the Lipkin operator	37
4.3.2	Symmetries in $f(\hat{O})$	38
4.3.3	Matrix elements of $f(\hat{O})$	38
4.3.4	Other approximate projection methods	39
5	Results	41
5.1	Uncertainty propagation	41
5.2	Symmetry restoration with the Lipkin method	44
6	Summary	49
A	Derivation of the relation (4.14)	51
B	Properties of kernels used in subsection 4.3.1	55

Chapter 1

Introduction

The efforts towards modeling the nuclear structure with high precision and sound physical meaning have been carried out for several decades. A large part of the representative results in this domain can be roughly divided into three types of methods [3, 4]:

1. The *ab initio* approaches that aim at building the wave function that describes the considered system from first principles. Examples of these approaches include the no-core shell model (NCSM) [5], coupled-cluster (CC) expansion method [6], and lattice effective field theory (LEFT) [7].
2. The macroscopic approaches such as the liquid drop model [8], in which the quantal effects are, at most, only partially described.
3. The configuration interaction model (CI) [9] and DFT [3, 10] that are quantal and microscopic but effective approaches.

The *ab initio* approaches, in principle, contain the least approximations. They are suitable for calculations of light nuclei. For example, the LEFT has been used to describe the Hoyle state in ^{12}C [7]. However, they are not tractable for heavier systems because of their large computational cost. The macroscopic approaches can only describe the bulk properties of nuclei, such as the binding energies on average. Compared with the macroscopic models, the CI and DFT are microscopic. Compared with the *ab initio* approaches, the approximations they use make them less computationally expensive. Typical CI approaches, such as the Shell Model (SM), can be used for calculations in nuclei up to the region around ^{132}Sn , while the DFT, which is the theoretical tool I use in this thesis, is currently the only branch of microscopic models that can be used to describe both medium-mass and heavy nuclei [11, 12].

The basic ingredient and degree of freedom used in the DFT is the 1-body density ρ of a system [13]. In this method, the energy E of a system is viewed as a functional of the 1-body density. The ground-state energy is obtained by minimizing this functional. In principle, as claimed by the Hohenberg-Kohn (HK) theorem, the energy density functional (EDF) for systems in different external fields but with the same kind of interaction between their constituents has a universal form. Thus, searching for this universal form is a natural goal in this method. Theoretically, one can determine the functional by exploring the whole $E \sim \rho$ plane using all kinds of external fields as Lagrange multipliers [14]. Since this is not doable, in practice, one builds a model EDF with the help of some approximations and phenomenology. The differences between the true universal density functional and the model EDFs indicate the necessity to improve results given

by the latter with the guidance of experimental data. For example, one can construct a simple EDF with particle-number and rotational symmetries by calculating the mean-field average of an EDF generator [15, 16]. Such simple EDFs can give overall satisfying descriptions for most of the nuclei, but improvements are certainly very much needed [4, 15, 17, 18].

To improve the calculated results obtained from the simple EDFs mentioned above, one can use two strategies:

1. Improving the EDF generator. One can develop new forms based on some mathematical and physical principles [19–21]. One can also optimize the parameters that appear in the EDF with the help of increasingly rich experimental data and growing computational power [22].
2. Generalizing the states that are used to calculate the averages of the EDF generator.

An example of the first strategy is to introduce higher-order terms into the EDF [23–26]. Methods based on symmetry breaking and symmetry restoration [27–29] belong to the second strategy [19]. Strategies of improving the results given by the EDF calculations are the main topic of this thesis.

Chapter 2

Density functional theory and mean-field method

In this chapter, I introduce the general concepts of the DFT and the framework of the SCMF method. I also discuss the EDF generators that are needed for meaningful SCMF calculations as well as possible improvements of mean-field results. DFT claims that the ground-state energy of an N -particle system corresponds to the minimum of a functional of its 1-body density. It can be used as the theoretical guideline for ground-state energy calculations. To find the practical form of this functional, one can build a model EDF from the so-called EDF generators [16] by calculating their mean-field averages. As this is an approximation, there are differences between the results given by the model EDF and experimental data [4, 15, 17, 18]. To improve the results, one can introduce the spontaneous-symmetry-breaking mechanism. A further improvement leads to the so-called beyond-mean-field methods.

2.1 General concepts of DFT

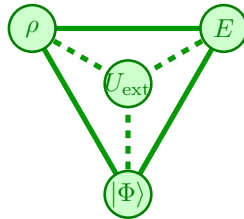


Figure 2.1: There are one-to-one mappings between the density ρ , ground state $|\Phi\rangle$, external potential U_{ext} , and ground-state energy E , provided the ground state of the considered system is non-degenerate.

One of the foundations of DFT is the Hohenberg-Kohn (HK) theorem [30]. Consider a system of N interacting fermions with a non-degenerate ground state. Its Hamiltonian can be written as

$$\hat{H} = \hat{T} + \hat{V} + \hat{U}_{\text{ext}}, \quad (2.1)$$

where \hat{T} is the kinetic energy term, \hat{V} is the two-body interaction term and \hat{U}_{ext} is the local external field. The 3-body and higher-order terms are ignored for simplicity. One can construct

a set \mathcal{U} of different \hat{U}_{ext} in which each \hat{U}_{ext} gives a non-degenerate ground state [31]:

$$\mathcal{U} = \left\{ \hat{U}_{\text{ext}} \mid \text{Give non-degenerate ground state } \hat{U}'_{\text{ext}} \neq \hat{U}_{\text{ext}} + \text{const} \right\}. \quad (2.2)$$

Here two \mathcal{U} that differ only by a constant are considered as the same. Keeping \hat{V} fixed, for each element in \mathcal{U} , one can determine a ground state $|\Psi\rangle$ of the system and construct two sets:

$$\mathcal{G} = \{ |\Psi\rangle \mid \text{Ground states corresponding to elements in } \mathcal{U} \}, \quad (2.3)$$

$$\mathcal{N} = \{ \rho_0 \mid \text{1-body ground-states density corresponding to elements in } \mathcal{G} \}. \quad (2.4)$$

The 1-body ground-state density is defined as

$$\rho_0(\mathbf{r}) = \sum_{\alpha_1 \cdots \alpha_N} \int d\mathbf{r}_2 \cdots d\mathbf{r}_N |(\mathbf{r}\alpha_1 \mathbf{r}_2 \alpha_2 \cdots \mathbf{r}_N \alpha_N | \Psi\rangle|^2 \quad (2.5)$$

with α the quantum numbers used to label the single-particle states.

As illustrated in Fig. 2.1, and according to the HK theorem, there are one-to-one mappings $f_{nu} : \mathcal{N} \rightarrow \mathcal{U}$ from set \mathcal{N} to set \mathcal{U} and $f_{ng} : \mathcal{N} \rightarrow \mathcal{G}$ to set \mathcal{G} . Therefore, a ground state $|\Psi_i\rangle$ in \mathcal{G} can be viewed as the value of a functional $|\Psi[\rho]\rangle$ at the corresponding 1-body ground-state density $\rho = \rho_{0,i}$, where $\rho_{0,i}$ is the counter image of $|\Psi_i\rangle$ under f_{ng} . Here i is used as a label of the group elements in sets \mathcal{N} , \mathcal{G} or \mathcal{U} . A similar statement holds for the external field $\hat{U}_{\text{ext},i}$ in \mathcal{U} . This means that the energy of ground state $|\Psi_i\rangle$ can be written as

$$\begin{aligned} E_{0,i} &= E[\rho_{0,i}] \\ &= F_{\text{HK}}[\rho_{0,i}] + \int d\mathbf{r} U_{\text{ext},i}(\mathbf{r}) \rho_{0,i}(\mathbf{r}), \\ F_{\text{HK}}[\rho_{0,i}] &\equiv \langle \Psi_i | \hat{T} + \hat{V} | \Psi_i \rangle, \end{aligned} \quad (2.6)$$

where F_{HK} is a universal functional. By definition, if \hat{U}_{ext} is fixed to $\hat{U}_{\text{ext},i}$, by solving the equation

$$\frac{\delta E[\rho(\mathbf{r})]}{\delta \rho(\mathbf{r})} = \mu, \quad (2.7)$$

one can find that the minimum is located at $\rho = \rho_{0,i}$ with $E[\rho_{0,i}(\mathbf{r})]$ the exact ground state energy. In Eq. (2.7), μ is a Lagrange multiplier coming from the constraint $\mu [\int d\mathbf{r} \rho(\mathbf{r}) - N] = 0$ on particle number.

Another important tool for the DFT is the Kohn-Sham (KS) scheme [32]. It states that for an N -particle interacting system, there exists a non-interacting KS system that has the same 1-body ground-state density as the original system. Let us write the Hamiltonian of the KS system as

$$\hat{H}_{ks} = \hat{T} + \hat{U}_{ks}. \quad (2.8)$$

By solving the single-particle equation

$$\left(-\frac{\hbar^2}{2m} \nabla^2 + U_{ks}(\mathbf{r}) \right) \phi_k(\mathbf{r}) = \epsilon_k \phi_k(\mathbf{r}), \quad (2.9)$$

one can obtain the single-particle orbits. Since the KS system is non-interacting, the ground state can be built by filling these orbits from the lowest to the highest so as to respect the

anti-symmetry requirement. Thus, it can be represented by a single Slater determinant. The 1-body ground-state density can be expressed as:

$$\rho_0 = \sum_{i=1}^N |\phi_i|^2. \quad (2.10)$$

\hat{U}_{ks} can be determined from the variational principle. Let the ground state of the KS system be $|\Phi\rangle$. Since the HK theorem also holds for a non-interacting system, there is $|\Phi\rangle = |\Phi[\rho_0]\rangle$. The ground-state energy of the original interacting system can be expressed as

$$E_0[\rho_0] = T[\rho_0] + \tilde{V}[\rho_0] + \tilde{V}_c[\rho_0], \quad (2.11)$$

where

$$\begin{aligned} T[\rho_0] &\equiv \langle \Phi[\rho_0] | \hat{T} | \Phi[\rho_0] \rangle, \\ \tilde{V}[\rho_0] &\equiv \langle \Phi[\rho_0] | \hat{V} + \hat{U}_{\text{ext}} | \Phi[\rho_0] \rangle, \\ \tilde{V}_c[\rho_0] &\equiv \langle \Psi[\rho_0] | \hat{H} | \Psi[\rho_0] \rangle - \langle \Phi[\rho_0] | \hat{H} | \Phi[\rho_0] \rangle, \end{aligned}$$

and \hat{H} and $|\Psi\rangle$ are the Hamiltonian and ground-state wave function of the interacting system. $E[\rho_0]$ can also be expressed as [31]

$$\begin{aligned} E_0[\rho_0] &= T[\rho_0] + E_H[\rho_0] + E_{\text{ext}}[\rho_0] + E_{xc}[\rho_0], \quad (2.12) \\ E_H[\rho_0] &\equiv \int d\mathbf{r}d\mathbf{r}' V(\mathbf{r}, \mathbf{r}') \rho(\mathbf{r}') \rho(\mathbf{r}) \\ E_{\text{ext}}[\rho_0] &\equiv \int d\mathbf{r} U_{\text{ext}}(\mathbf{r}) \rho(\mathbf{r}) \\ E_{xc}[\rho_0] &\equiv \langle \Psi | \hat{T} + \hat{V} | \Psi \rangle - E_H[\rho_0] - T[\rho_0]. \end{aligned}$$

Eq. (2.12) is the common expression in electronic DFT. By applying the variational principle [15], one gets

$$\begin{aligned} \delta E_0|_{\rho=\rho_0} &= \left[\langle \delta\Phi | \hat{T} | \Phi \rangle + \langle \Phi | \hat{T} | \delta\Phi \rangle + \delta\tilde{V} + \delta\tilde{V}_c \right]_{\rho=\rho_0} \\ &= \left[\delta\tilde{V} + \delta\tilde{V}_c - \sum_i \frac{\hbar^2}{2m} \int d\mathbf{r} \delta\phi_i^* \nabla^2 \phi_i + \phi_i^* \nabla^2 \delta\phi_i \right]_{\rho=\rho_0} \\ &= \left[\delta\tilde{V} + \delta\tilde{V}_c + \sum_i \epsilon_i \delta \left(\int d\mathbf{r} (\phi_i^* \phi_i) \right) - \int d\mathbf{r} U_{ks} \delta \left(\sum_i (\phi_i^* \phi_i) \right) \right]_{\rho=\rho_0} \quad (2.13) \\ &= \left[\delta\tilde{V} + \delta\tilde{V}_c - \int d\mathbf{r} U_{ks} \delta\rho \right]_{\rho=\rho_0} \\ &= 0 \end{aligned}$$

In Eq. (2.13), the single-particle equation (2.9) and orthonormality of the single-particle orbitals are used. The Lagrange multiplier is dropped since it only shifts the results by a constant. Because Eq. (2.13) should hold for any $\delta\rho$, one has

$$U_{ks} = \frac{\delta\tilde{V}}{\delta\rho} + \frac{\delta\tilde{V}_c}{\delta\rho}. \quad (2.14)$$

In principle, if the form of the energy density functional $E_0[\rho]$ is known, one can construct the proper KS system to calculate the 1-body ground-state density and thus the ground-state energy. However, in practical, this form is difficult to obtain and approximations are needed. The self-consistent mean-field method can be viewed as one of the possible approximations [19].

2.2 SCMF method in nuclear system

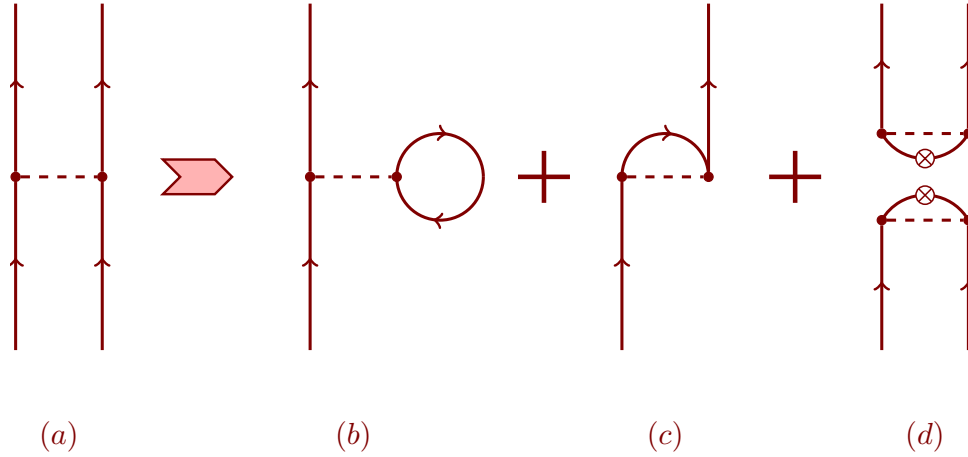


Figure 2.2: By using the Wick theorem and variational principle, the two-body interaction is transformed into a sum of one-body density-dependent potentials: (a) and (b) represent self-consistent mean fields at the Hartree-Fock level; (c) appears when pairing is activated and pairs are allowed to be created (upper part of (c)) and annihilated (lower part of (c)).

2.2.1 The EDF from the Hartree-Fock average

For an interacting many-nucleon system, ignoring for simplicity the 3-body and higher-order interactions, one can write the Hamiltonian as

$$\hat{H} = \hat{T} + \hat{V} = \sum_{ij} t_{ij} c_i^\dagger c_j + \frac{1}{4} \sum_{ijkl} \bar{v}_{ijkl} c_i^\dagger c_j^\dagger c_l c_k \quad (2.15)$$

with c^\dagger , c being the creation and annihilation operators of a complete set of basis states and \bar{v}_{ijkl} the anti-symmetrized matrix elements of the interaction. In the self-consistent mean-field (SCMF) treatment of nuclei, a nucleus with N nucleons is approximated by a non-interacting system with the same number of independent fermions moving in the field built by nucleons themselves. This assumption is supported by experimental evidence such as the existence of magic numbers [15].

As the eigenstates of the Hamiltonian of the non-interacting system, all single-particle orbits of the non-interacting system form a complete orthogonal set. The creation operator a_l^\dagger corresponding to the single-particle state $|l\rangle$ can always be obtained by applying a unitary transformation on an arbitrary complete orthogonal set c^\dagger

$$a_l^\dagger = \sum_k D_{lk} c_k^\dagger, \quad (2.16)$$

where D is a matrix representing the transformation. As what one has done in the KS system, the ground state of the non-interacting system $|\Phi\rangle$ can be constructed by filling particles from the lowest to highest orbit so as to respect the Pauli principle:

$$|\Phi\rangle = |\text{MF}\rangle = \prod_{i=1}^N a_i^\dagger |-\rangle. \quad (2.17)$$

In the above, $|-\rangle$ is the bare vacuum. It is clear that the state $|\text{MF}\rangle$ here has good particle number and has the form of a product state. From the Wick theorem [33], one gets

$$\begin{aligned} \langle \text{MF} | c_i^\dagger c_j^\dagger c_l c_k | \text{MF} \rangle &= \rho_{ki} \rho_{lj} - \rho_{li} \rho_{kj}, \\ \rho_{ki} &\equiv \langle \text{MF} | c_i^\dagger c_k | \text{MF} \rangle \\ &= \sum_{j=1}^N D_{kj} D_{ij}^\dagger. \end{aligned} \quad (2.18)$$

In Eq. (2.18), ρ_{ij} is the density matrix. Since D is a unitary matrix, the density matrix satisfies the condition $\rho^2 = \rho$ and is a projection operator. The average (Hartree-Fock average) value of the Hamiltonian defined in Eq. (2.15) under the mean-field ground state can be expressed as

$$E_{0,\text{MF}} = \langle \text{MF} | \hat{H} | \text{MF} \rangle = \sum_{ij} t_{ij} \rho_{ji} + \frac{1}{2} \sum_{ijkl} \bar{v}_{ijkl} \rho_{ki} \rho_{lj}. \quad (2.19)$$

The fact that \bar{v}_{ijkl} is antisymmetric is used to obtain this expression.

One immediately sees that the EDF $E_{0,\text{MF}}$ is expressed as a functional of the matrix ρ . From the HK theorem, one knows that this matrix should also be a functional of the 1-body density. On the other hand, because of the form of the ground state, the 2-body density matrix $\langle \Phi | c_i^\dagger c_j^\dagger c_l c_k | \Phi \rangle$, which is another functional of the 1-body density, is replaced by simple products of 1-body density matrices. Since in general case this replacement doesn't always hold, the dependence of this EDF on the 1-body density is restricted to some degree.

2.2.2 SCMF equation

The minimum of $E_{0,\text{MF}}$ can be found by using the variational principle. The variational equation is

$$\sum_{ij} \frac{\delta}{\rho_{ij}} \{ E_{0,\text{MF}} - \text{Tr} [\Lambda (\rho^2 - \rho)] \} \delta \rho_{ij} = 0. \quad (2.20)$$

where Λ is a parameter matrix. The term

$$\text{Tr} [\Lambda (\rho^2 - \rho)] = \sum_{ij} \Lambda_{ij} \left(\sum_k \rho_{jk} \rho_{ki} - \rho_{ji} \right) \quad (2.21)$$

is introduced to keep ρ a projection operator. This is necessary if one wants to keep the correspondence between the state described in Eq. (2.17) and density matrix [15]. After some

calculations, one can get rid of Λ and obtain the SCMF equation:

$$\begin{aligned} [h, \rho] &= 0, \\ h_{ij} &\equiv \frac{\delta E_{0,\text{MF}}}{\delta \rho_{ji}} = t_{ij} + \Gamma_{ij}, \\ \Gamma_{ij} &= \sum_{kl} \bar{v}_{ijkl} \rho_{lk}. \end{aligned} \quad (2.22)$$

In the above equation, Γ_{ij} corresponds to (a) and (b) in Fig. 2.2. It is just the mean field created by the particles themselves. This equation shows that h and ρ can be diagonalized simultaneously when the matrix D in Eq. (2.18) corresponds to the set of single-particle orbits that minimizes the energy. Because D must always diagonalize ρ , one should try to find the transformation that can diagonalize h . Thus, the SCMF equation can also be written as

$$\sum_k h_{ik} D_{kj} = D_{ij} \epsilon_j, \quad (2.23)$$

where ϵ_j is the j^{th} eigenvalue of h .

2.2.3 The EDF Generator

The bare nucleon-nucleon (NN) force can be extracted from NN scattering data and has a strong repulsive core at short range [34]. This means that its matrix elements can be very large. In order to get a finite expectation value for the Hamiltonian in Eq. (2.15), the amplitude of the wave function of the system should become small enough when two particles become close to each other. For example, one can consider a bare NN force with a hard core. The force goes to infinity when the distance r between any two particles is smaller than the radius of the hard core $r_c \approx 0.4$ fm [15]. Thus the wave function must be 0 when r is smaller than r_c . This indicates that the wave function is correlated and, therefore, it is difficult, if not impossible, to express it as a product state. In other words, in nuclear physics, the correction term \tilde{V}_c in Eq. (2.11) is too large to be ignored. But if one uses the bare nuclear force in Eq. (2.15), this term is completely missing in the obtained $E_{0,\text{MF}}$.

To overcome this problem, one can replace the interaction part of the nuclear Hamiltonian by the so-called EDF generator \hat{G} [16]. This replacement is reasonable since the Hamiltonian is only used to generate the EDF. It is the density and EDF that are used to solve the ground-state-energy problem. By this replacement, one hopes that at least the major part of \tilde{V}_c can be included in the generated EDF. A phenomenological way to determine \hat{G} is to formulate it as

$$\hat{G} = \sum_i C_i \hat{O}_i, \quad (2.24)$$

where \hat{O}_i are some two-body, three-body, etc., operators and C_i are coupling constants that should be adjusted to minimize the difference between theoretical results and experimental data. Operators appearing in Eq. (2.24) are usually restricted by symmetries that exist in the nuclear force. For example, they need to be invariant under rotation in coordinate space, under Galilean transformation, etc [15]. The EDF created from \hat{G} in Eq. (2.24) is a modelisation/approximation of the exact EDF. One can call it a model EDF. Examples of the EDF generators are the Skyrme interaction [35–38] and Gogny interaction [39].

The Skyrme force that is used in article I and II is an important EDF generator. It has the following form:

$$\begin{aligned}
\hat{v} = & t_0 \left(1 + x_0 \hat{P}_\sigma\right) \delta(\mathbf{r}_{12}) \\
& + \frac{1}{2} t_1 \left(1 + x_1 \hat{P}_\sigma\right) \left[\hat{\mathbf{k}}^\dagger \delta(\mathbf{r}_{12}) + \delta(\mathbf{r}_{12}) \hat{\mathbf{k}}^2\right] \\
& + t_2 \left(1 + x_2 \hat{P}_\sigma\right) \hat{\mathbf{k}}^\dagger \cdot \delta(\mathbf{r}_{12}) \hat{\mathbf{k}} \\
& + \frac{1}{6} t_3 \left(1 + x_3 \hat{P}_\sigma\right) \delta(\mathbf{r}_{12}) \rho^\alpha(\mathbf{R}) \\
& + iW_0 (\hat{\boldsymbol{\sigma}}_1 + \hat{\boldsymbol{\sigma}}_2) \cdot \hat{\mathbf{k}}^\dagger \times \delta(\mathbf{r}_{12}) \hat{\mathbf{k}}.
\end{aligned} \tag{2.25}$$

In Eq (2.25), $\hat{P}_\sigma = \frac{1}{2} (1 + \hat{\boldsymbol{\sigma}}_1 \cdot \hat{\boldsymbol{\sigma}}_2)$ is the spin-exchange operator, \mathbf{r}_{12} is the distance between two particles, and $\hat{\mathbf{k}} = -\frac{i}{2} (\nabla_1 - \nabla_2)$ is the relative momentum operator. The first three terms can be viewed as the leading-order and next-to-leading-order terms of the Taylor expansion of a nuclear force in the momentum space. The fourth term is the density-dependent term. The last term represents a spin-orbit interaction. In each term, there are two ($t_i, x_i, i = 1, 2, 3$) or one (W_0) coefficients. They are corresponding to the coupling constants C_i in Eq. (2.24). Until now, there are already many sets of Skyrme parameterizations available in the literature, see Ref [40].

Since the Skyrme force is a zero-range interaction, the resulting Skyrme EDF [41] contains only the local and quasi-local terms. Local terms are terms constructed from the diagonal elements of the density matrix in the coordinate space. They come from the first and fourth terms of the Skyrme force. Quasi-local terms are constructed by acting with the gradient operator on the density matrix in the coordinate space before taking its diagonal elements. They come from the second, third, and last terms of the Skyrme force. Because the Skyrme EDF has only the local and quasi-local terms, the mean field derived from it also has only the local and quasi-local terms.

2.2.4 S-SC-MF-EDF calculation

By using the product state, EDF generator, and some symmetry constraints, one can build a standard symmetry-conserving mean-field EDF (S-SC-MF-EDF). By the standard, I mean that the standard EDF generator, such as the Skyrme interaction, is used to generate the EDF. By the symmetry-conserving mean field, I mean that the used product state carries all possible symmetries that come from the Hamiltonian. Examples of these symmetries are the particle-number symmetry and rotational symmetry. The reason of adding the symmetry constraints is that one may want to obtain the ground-state energy and real 1-body ground-state density which has all possible symmetries at the same time. This is, at least in principle, possible because of the HK theorem.

After the EDF is generated, with the help of the SCMF equation, the ground-state energy as well as the density matrix can be calculated. The whole process is summarized in Fig. 2.3. As demonstrated in the figure, the SCMF equation is solved iteratively. This is because the equation is non-linear. The non-linear property comes from the fact that the matrix h depends on the transformation matrix D , which is in turn the solution of this equation.

Once the results are obtained, one can compare them to experimental data. Because the S-SC-MF-EDF is only a modelisation/approximation to the exact EDF, one should expect some

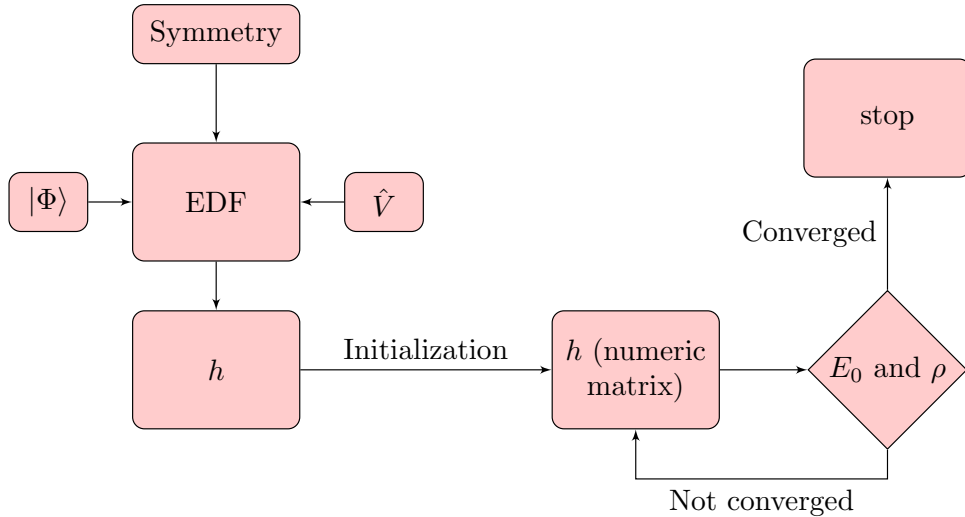


Figure 2.3: The process of a S-SC-MF-EDF calculation

differences between its results and exact ones. In fact, in most case, the comparisons show that the S-SC-MF-EDF calculation is not good enough. For example, for ^{240}Pu , the binding energy difference between the experiment and calculation can be around 20 MeV [4] (2 percent of the total binding energy). Also, some observed facts, such as the energy gap in even-even nuclei and odd-even effect in odd-even nuclei cannot be described by this EDF. To overcome these problems, one should search for methods to improve it.

2.3 Possible improvements

Since one important source (if not the only source) of the difference between the S-SC-MF-EDF results and experimental data is the imperfection of the model EDF, and the model EDF is generated by the EDF generator, one natural way to improve the calculated results is to improve the EDF generators. Besides modifying the generator, generalizing the state $|\text{MF}\rangle$ is also one way for improvement.

2.3.1 Improving the EDF generator

In order to construct an EDF generator, one first constructs a function of operators that contains some unknown parameters and then adjusts these parameters to experimental data. From this process, one can see that the form of the function and its parameters are two basic elements of the EDF generators. Thus, to improve them, one can use two methods:

1. Optimizing the parameters to experimental data and improving the fitting procedure [22]. By doing this, one can constrain the parameters better and absorb more corrections corresponding to the missing part in the model EDF into the parameters.
2. Adding/Changing terms in the EDF generator with the guidance of physical and mathematical principles so that one can create a better approximation of the exact EDF [19].

Of course, one can also combine these two aspects together, that is, to optimize the parameters of a modified EDF generator.

2.3.2 Generalizing the state

From subsection 2.2.4, one sees that the state $|\text{MF}\rangle$ used in S-SC-MF-EDF is constrained by the symmetry-conserving requirement and by the single Slater determinant form of the wave function. By removing these constraints, one can enlarge the subset used to search for the minimum of Eq. (2.20) in the Hilbert space, which may lower the calculated ground-state energy. If the symmetry-conserving requirement is removed, the spontaneous symmetry breaking (SSB) [42] is introduced into the calculation. This strategy is widely used in the mean-field calculations nowadays. If one turns to the superposition of Slater determinants [4], the calculation goes towards including the so-called beyond-mean-field effects. Examples are the generator coordinate method (GCM) and projection method, where the latter is a special case of the former, and it is used to restore broken symmetries. Since the Lipkin method discussed in article II is related to the symmetry restoration, here I only give a brief introduction to the SSB mechanism and projection method.

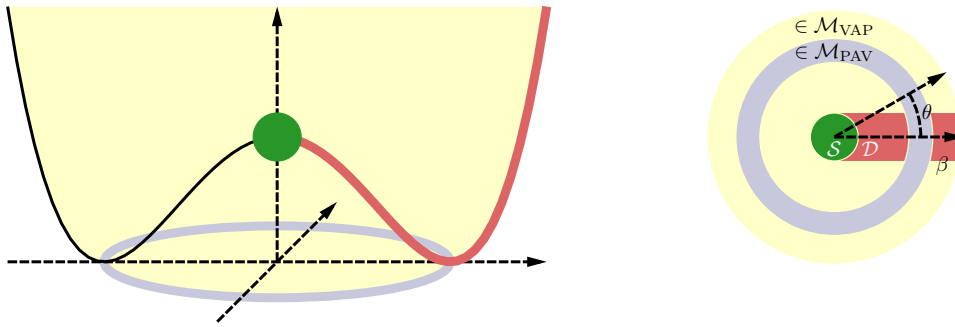


Figure 2.4: A schematic diagram of the SSB in the rotational symmetry and angular momentum projection. β denotes the deformation; θ is the orientation of the wave function. The green dot is the subset \mathcal{S} of Hilbert space containing spherical product states. The red line is the subset \mathcal{D} that includes both spherical and deformed product states. The blue circle represents the set of basis on which the subspace used in the PAV method is expanded. Each circle in the yellow region is a set of basis used to expand a subspace. The union of these subspaces is the subset used in the VAP method.

Spontaneous Symmetry Breaking

Consider a Hamiltonian that has a given symmetry S . One can minimize the energy in a subset \mathcal{S} of the Hilbert space that only contains product states having the symmetry S so that the solution always has this symmetry. But because of possible SSB, a product state without the symmetry S may give a lower energy. In order to get a better ground state, one often needs to extend the subset \mathcal{S} to a subset \mathcal{D} that contains at least part of the product states that break the symmetry S .

Take the rotational symmetry of nuclei as an example. One can search for the ground state in the subset which only contains product states that are invariant under arbitrary rotations.

This would give a spherical ground state that preserves the rotational symmetry. But if one also includes deformed product states in the subset, it is common that the ground state of a nucleus having non-magic neutron and proton numbers is among these deformed states. This is because when the symmetry restriction is removed, the contributions from the quadrupole part and possibly from other higher-order parts of the interaction are no longer zero. They can lower the ground-state energy and drive the nucleus towards deformation. For more detailed explanations, see Ref [15].

Besides the rotational symmetry, particle-number symmetry is another symmetry that is often broken. The method used to break the particle-number symmetry is the Bogoliubov transformation [15, 43]. By breaking this symmetry, a non-interacting quasiparticle system without good particle number is used to approximate the N -particle interacting system.

The SCMF calculation without particle-number symmetry is summarized in Table 2.1 and compared with the situation where this symmetry is conserved. As demonstrated in the table, in the case without particle-number symmetry, the creation and annihilation operators of the non-interacting quasiparticle system (β^\dagger and β) are linked with those of a complete single-particle basis (c^\dagger and c) by the unitary Bogoliubov transformation \mathcal{W} . The ground state is constructed by annihilating all quasiparticles in the bare vacuum. It is then a product state. Since the transformation can lead to mixing between particle creation and annihilation operators, the ground state now does not always have good particle number. As a consequence of breaking this symmetry, new terms containing the pairing tensor κ are introduced into the EDF.

Because \mathcal{W} is unitary, the general density matrix \mathcal{R} instead of ρ is now a projection operator. By replacing ρ explicitly appearing in Eq. (2.20) by \mathcal{R} and adding the term $\lambda \text{Tr} \rho$, one gets the variational equation for the EDF in the particle-number-symmetry-breaking case. The additional term is used to constrain the particle number so that it is equal to N . Similar to Eq. (2.22), the mean-field equation now shows that by diagonalizing the matrix \mathcal{H} , one can find the transformation \mathcal{W} that minimizes the ground-state energy.

Usually, the symmetry breaking can contribute up to 2% of the total binding energy [4]. What's more, by breaking the particle-number symmetry, one can include the effect of pairing correlations (the short-range correlations between two particles coupled to $J = 0$ pairs). This leads to a generally successful description of the phenomena such as the energy gap in even-even nuclei, the odd-even effect, etc.

Although the symmetry breaking can improve the results of the calculations, it also has some disadvantages. First, as a finite self-bound system, the real ground state should carry all possible symmetries of the Hamiltonian [15]. For example, the axial deformation of a nucleus is smeared out by the fact that its symmetry axis can point to any direction with equal probability. This indicates that one can lower the calculated ground-state energy by restoring the symmetry. In addition, because of the symmetry breaking, the 1-body ground-state density given by symmetry-unrestricted mean-field EDF calculation is not the true density. Thus this kind of calculation does not actually stay in the frame of the HK theorem [4]. In nuclear physics, there are already some efforts to link the symmetry-broken density to the density in the intrinsic frame of the nucleon and to build a HK-like theorem and a KS scheme inside this frame [44, 45]. Moreover, some quantities can only be calculated with states that have good quantum numbers. For example, the transition probabilities [18] are defined between states with good total angular momentum. It is meaningless to calculate them between states without rotational symmetries. To solve these problems, one should restore the symmetries.

Method	SCMF+particle-number symmetry	SCMF+particle-number symmetry breaking
Creation and annihilation operators	$\begin{bmatrix} a \\ a^\dagger \end{bmatrix} = \begin{bmatrix} D^\dagger & 0 \\ 0 & D^T \end{bmatrix} \begin{bmatrix} c \\ c^\dagger \end{bmatrix}, D \text{ is unitary.}$	$\begin{bmatrix} \beta \\ \beta^\dagger \end{bmatrix} = W^\dagger \begin{bmatrix} c \\ c^\dagger \end{bmatrix}, W = \begin{bmatrix} U^\dagger & V^\dagger \\ V^T & U^T \end{bmatrix}$ is unitary.
Ground State	$ \Phi\rangle = \prod_{i=1}^N a_i^\dagger -\rangle$	$ \Phi\rangle = \prod_k \beta_k -\rangle$ k goes over all quasiparticles in the bare vacuum.
EDF	$E_{0, \text{MF}} = \text{Tr} [t\rho] + \frac{1}{2} \text{Tr} \text{Tr} [\rho \bar{v} \rho]$ $\rho_{ji} = \langle \Phi c_i^\dagger c_j \Phi \rangle$	$E_{0, \text{MF}} = \text{Tr} [t\rho] + \frac{1}{2} \text{Tr} \text{Tr} [\rho \bar{v} \rho] + \frac{1}{4} \text{Tr} \text{Tr} [\kappa^* \bar{v} \kappa]$ $\rho_{ji} = \langle \Phi c_i^\dagger c_j \Phi \rangle, \kappa_{ji} = \langle \Phi c_i c_j \Phi \rangle$
Projection operator	$\rho = DD^\dagger = \rho^2$	$\mathcal{R} = \begin{pmatrix} V^* \\ U^* \end{pmatrix} \begin{pmatrix} V^T & U^T \end{pmatrix} = \begin{pmatrix} \rho & \kappa \\ -\kappa^* & 1 - \rho^* \end{pmatrix} = \mathcal{R}^2$
Variational equation	$\sum_{ij} \frac{\delta}{\delta \rho_{ij}} \{ E_{0, \text{MF}} - \text{Tr} [\Lambda (\rho^2 - \rho)] \} \delta \rho_{ij} = 0$	$\sum_{ij} \frac{\delta}{\delta \mathcal{R}_{ij}} \{ E'_{0, \text{MF}} - \text{Tr} [\Lambda (\mathcal{R}^2 - \mathcal{R})] \} \delta \mathcal{R}_{ij} = 0$ $E'_{0, \text{MF}} = E_{0, \text{MF}} - \lambda \text{Tr} \rho$ λ is determined by the condition $\text{Tr} \rho = N$.
Mean-field equation	$[h, \rho] = 0 \Leftrightarrow hD = DE$ $h = t + \Gamma, \Gamma_{ij} = \frac{1}{2} \sum_{lk} \bar{v}_{ikj} i \rho_{lk}$ $E = \text{diag} \{ \epsilon_i \}$ is a diagonal matrix.	$[\mathcal{H}, \mathcal{R}] = 0 \Leftrightarrow \mathcal{H} \mathcal{W} = \mathcal{W} \mathcal{E}$ $\mathcal{H} = \begin{pmatrix} h - \lambda & \Delta \\ -\Delta^* & -h^* + \lambda \end{pmatrix}, \Delta_{ij} = \frac{1}{4} \sum_{lk} \bar{v}_{ijkl} \kappa_{kl},$ $\mathcal{E} = \begin{pmatrix} E & 0 \\ 0 & -E \end{pmatrix}$ is a diagonal matrix.

Table 2.1: Comparison between SCMF calculations with and without the particle-number symmetry

Restoring symmetries by Projection

By saying “Restoring the symmetry S ”, one means that one wants to build eigenstates that belong to irreducible representations of the symmetry group. To restore the symmetry, one can move from \mathcal{D} to some subset \mathcal{M} where superpositions of product states are also included. If \mathcal{M} is invariant under the elements of the symmetry group, it can be shown that in this subset the energy minimization can be achieved while requiring the states to have the proper symmetry [15].

Let us take the particle-number restoration as an example. The generator of the symmetry group is the particle-number operator \hat{N} . The eigenstates of this operator are what one wants to build by projection. The element of the symmetry group is $\hat{R}(\theta) = \exp[-i\hat{N}\theta]$, where θ is a parameter called the gauge angle.

Now consider an N -fermion system. Assume E_{model} is used to approximate the exact EDF of the system. It is generated by some model Hamiltonian \hat{H}_{model} that commutes with the particle-number operator. By performing the SCMF calculation with particle-number symmetry breaking, one can obtain a particle-number-symmetry-breaking ground state $|\Phi\rangle$ at the mean-field level. With the help of the symmetry group elements, one can build a state

$$\begin{aligned} |K\rangle &= \int_0^{2\pi} d\theta \exp(-iK\theta) \hat{R}(\theta) |\Phi\rangle \\ &\equiv \hat{P}^K |\Phi\rangle, \end{aligned} \quad (2.26)$$

where K is an integer. By writing $|\Phi\rangle$ as a superposition of states with good particle numbers, it is easy to show that $|K\rangle$ is the eigenstate of the particle-number operator and has the eigenvalue K . Thus one can say that the operator \hat{P}^K projects out the eigenstate $|K\rangle$ from $|\Phi\rangle$. Since here the projection is done after the ground state is obtained by the variational principle, one refers to this strategy as “Projection After Variation” (PAV). Obviously, $|K\rangle$ is a state in the space expanded by the basis $\hat{R}(\theta) |\Phi\rangle$. One can write this space as \mathcal{M}_{PAV} . Since \hat{H}_{model} commutes with particle-number operator, state $|K=N\rangle$ is the eigenstate of \hat{H}_{model} in \mathcal{M}_{PAV} with correct particle number.

Another strategy of projection is the so-called “Variation After Projection” (VAP) method. In this method, one needs to solve the variational equation

$$\delta \frac{\langle \Phi | \hat{P}^N \hat{H}_{\text{model}} \hat{P}^N | \Phi \rangle}{\langle \Phi | \hat{P}^N \hat{P}^N | \Phi \rangle} = 0, \quad (2.27)$$

where $|\Phi\rangle$ is an arbitrary product state without good particle number. From Eq.(2.27), one sees that in VAP, one builds states with particle number N from many mean-field states, then selects the one with the lowest energy. On the other hand, in PAV, only the mean-field ground state is used to construct a particle-number-conserving state. Thus, VAP is superior to PAV in the sense that it searches for the minimum in a larger subset of the whole Hilbert space.

A more complicated example is the rotational-symmetry restoration. Assume one has at one’s disposal a triaxially deformed mean-field ground state. It is a mixture of components with good total-angular-momentum quantum number J and good magnetic quantum number M . In the frame of the PAV method, a state with good J and M values can be constructed from a

deformed mean-field ground state $|\Phi\rangle$ in the following way:

$$\begin{aligned} |JM\rangle &= \sum_K g_K \hat{P}_{MK}^J |\Phi\rangle = \sum_K g_K \sum_\alpha |JM\alpha\rangle \langle JK\alpha | \Phi\rangle \\ &= \sum_K g_K \frac{2J+1}{8\pi^2} \int d\Omega D_{MK}^{J*}(\Omega) \hat{R}(\Omega) |\Phi\rangle. \end{aligned} \quad (2.28)$$

In the above equation, α represents quantum numbers used to label states with same J and M . D_{MK}^{J*} is the Wigner function. $\hat{R}(\Omega)$ is the rotational symmetry group element and g_K is a parameter. g_K appears because now by using \hat{P}_{MK}^J operators with different K values one can build multiple states with the same J and M values from $|\Phi\rangle$. Since the matrix of the model Hamiltonian between them is not diagonal, the eigenstate of H_{model} in \mathcal{M}_{PAV} must be a mixture of them. To determine g_K , one can solve the generalized eigenvalue problem

$$\begin{aligned} \sum_{K'} h_{KK'}^J g_{K'} &= E^J \sum_{K'} n_{KK'}^J g_{K'}, \\ h_{KK'}^J &= \langle \Phi | \hat{P}_{MK}^{J\dagger} \hat{H}_{\text{model}} \hat{P}_{MK'}^J | \Phi \rangle = \langle \Phi | \hat{H}_{\text{model}} \hat{P}_{KK'}^J | \Phi \rangle, \\ n_{KK'}^J &= \langle \Phi | \hat{P}_{KK'}^J | \Phi \rangle. \end{aligned} \quad (2.29)$$

Obviously, by using operator \hat{P}_{MK}^J with different J values and by solving Eq. (2.29), one can obtain not only the ground state but also excited states in \mathcal{M}_{PAV} . This means that the projection method can be used as a tool of studying spectra of nuclei.

Since the wave functions used in the projection method become more complicated than those used in SCMF calculations, the projection method can be very time-consuming.

Chapter 3

Propagation of uncertainties

An effective model, such as the Skyrme EDF, basically contains some simplifying assumptions and a set of parameters which are adjusted to experimental data. As fitted to experimental data, these parameters must have uncertainties. These uncertainties propagate into the observables calculated by the model and become one part of the uncertainties of the latter, namely, the statistical errors. Another component of the uncertainty of a calculated observable is the systematic error. It comes from the fact that there are unknown missing elements in the used model. If the exact model is unknown, which is true in most cases in nuclear physics, it is difficult to calculate this type of errors. Compared with the systematic error, the statistical error is relatively easier to study with the help of the statistical analysis. By analyzing the statistical errors in the calculated results, one can explore the quality and predictive power of the used parameters. For example, the statistical errors of the calculated observables can be used to examine whether the results are accurate enough or not. By comparing the uncertainties with fit residuals (the differences between experimental data and theoretical results), one can estimate the effectiveness of changing the parameters within their uncertainties on improving theoretical results. By exploring how sensitively the value of a calculated observable reacts to a change of a given parameter, it is possible to determine whether the experimental data for this observable can help us to refine this parameter or not. Due to the reasons listed above, recently there have been numerous studies of theoretical uncertainties related to modeling nuclear phenomena [46–50]. Article I is among them. In this chapter, I recall the method used in article I. Some useful details that are not included in that article are also given.

3.1 The equations of propagation of uncertainties

As discussed in Sec. II of article I and in the above, the statistical errors of the theoretical results of observables are caused by the uncertainties in the model parameters. For an observable y which is a nonlinear function of a set of n parameters $\mathbf{x} = (x_1, \dots, x_n)^T$, the square of its

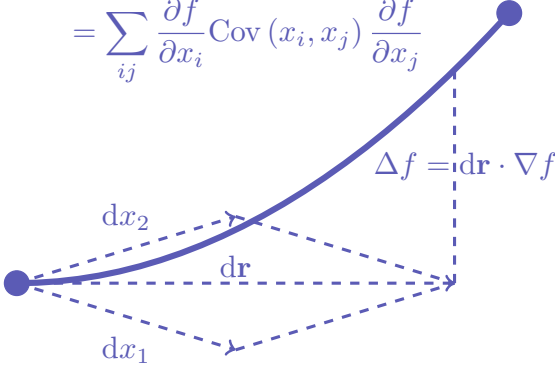
$$\begin{aligned}\sigma_f^2 &\equiv \langle \Delta f^2 \rangle - \langle \Delta f \rangle^2 \\ &= \sum_{ij} \frac{\partial f}{\partial x_i} \text{Cov}(x_i, x_j) \frac{\partial f}{\partial x_j}\end{aligned}$$


Figure 3.1: This figure demonstrates the equation of uncertainty propagation. If the function f can be approximated by the first-order Taylor polynomial at a point, the square of its standard error at this point can be expressed by the partial derivatives and covariant matrix of its parameters.

statistical error at $\mathbf{x} = \mathbf{x}_0$ can be calculated with the help of linearization:

$$\begin{aligned}\sigma_y^2|_{\mathbf{x}=\mathbf{x}_0} &= \text{E} [y - \text{E}(y)]^2|_{\mathbf{x}=\mathbf{x}_0} \\ &\approx \text{E} \left[y(\mathbf{x}) - y(\mathbf{x}_0) + \frac{\partial y}{\partial \mathbf{x}} \cdot (\mathbf{x} - \mathbf{x}_0) - \frac{\partial y}{\partial \mathbf{x}} \cdot \text{E}(\mathbf{x} - \mathbf{x}_0) \right]^2|_{\mathbf{x}=\mathbf{x}_0} \\ &= \sum_{i,j=1}^n \frac{\partial y}{\partial x_i} \frac{\partial y}{\partial x_j} \text{E}([x_i - \text{E}(x_i)][x_j - \text{E}(x_j)])|_{\mathbf{x}=\mathbf{x}_0} \\ &= \sum_{i,j=1}^n \frac{\partial y}{\partial x_i} \text{Cov}(x_i, x_j) \frac{\partial y}{\partial x_j}|_{\mathbf{x}=\mathbf{x}_0}.\end{aligned}\quad (3.1)$$

In the above, $\text{Cov}(x_i, x_j)$ is the covariance matrix of the parameters. It can be obtained in several approximate ways when doing the fitting [51]. For example, one can estimate the parameters by minimizing the sum of squared errors

$$\chi^2(\mathbf{x}) = \frac{1}{m-n} \sum_{i=1}^m [y_i(\mathbf{x}) - z_i]^2, \quad (3.2)$$

where $z_{i=1,\dots,m}$ are m measured values and $y_{i=1,\dots,m}$ are the corresponding calculated values depending on parameters \mathbf{x} . With the help of the Taylor expansion up to linear terms, and by assuming that the statistical errors of all z_i s are independent from each other and obey the normal distribution $N(0, \sigma^2)$, one can show that after the minimization is finished at $\mathbf{x} = \hat{\mathbf{x}}$, the covariance matrix of the parameters can be approximated by:

$$\text{Cov}(\hat{\mathbf{x}}, \hat{\mathbf{x}}) \approx \chi^2(\hat{\mathbf{x}}) (\mathbf{J}^T \mathbf{J})^{-1}, \quad J_{ij} = \frac{\partial y_i(\mathbf{x})}{\partial x_j}|_{\mathbf{x}=\hat{\mathbf{x}}}. \quad (3.3)$$

The derivatives of y are also needed in the uncertainty propagation formula. Since the dependence of the observables on the parameters can be quite complex, numerical methods are

needed. In our work, the Richardson extrapolation method [52] is used. For a function $f(a)$ and a finite step length h , $f'(a)$ can be approximated by a function $G_m(a, h)$. Its definition is

$$\begin{aligned} G_0(a, h) &= \frac{f(a+h) - f(a-h)}{2h}, \\ G_m(a, h) &= \frac{4^m G_{m-1}(h/2) - G_{m-1}(h)}{4^m - 1}, \end{aligned} \quad (3.4)$$

where $m = 1, 2, \dots$. By using induction, one can prove the relation between G_m and f' :

$$f'(a) - G_m(a, h) = O(h^{2(m+1)}). \quad (3.5)$$

3.2 Transformation between parameter sets

In article I, we used time-even Skyrme EDF and UNEDF0 parametrization for all calculations. The form of this EDF is [22]:

$$\begin{aligned} \mathcal{E}(\mathbf{r}) &= \sum_{t=0,1} \chi_t(\mathbf{r}) + \tilde{\chi}(\mathbf{r}), \\ \chi_t(\mathbf{r}) &= \sum_{t=0,1} \left[C_t^{\rho\rho} \rho_t^2(\mathbf{r}) + C_t^{\rho\tau} \rho_t(\mathbf{r}) \tau_t(\mathbf{r}) + C_t^{J^2} \mathbb{J}_t^2(\mathbf{r}) \right. \\ &\quad \left. + C_t^{\rho\Delta\rho} \rho_t(\mathbf{r}) \Delta\rho_t(\mathbf{r}) + C_t^{\rho\nabla J} \rho_t(\mathbf{r}) \nabla \cdot \mathbf{J}_t(\mathbf{r}) \right], \\ \tilde{\chi}(\mathbf{r}) &= \sum_{q=\frac{1}{2}, -\frac{1}{2}} \frac{V_0^q}{2} \left[1 - \frac{\rho_0(\mathbf{r})}{2\rho_{00}} \right] \tilde{\rho}_q \tilde{\rho}_q^*(\mathbf{r}), \\ C_t^{\rho\rho} &= C_{t0}^{\rho\rho} + C_{tD}^{\rho\rho} \rho_0^\gamma, \end{aligned} \quad (3.6)$$

where $q = \frac{1}{2}(-\frac{1}{2})$ represents neutron(proton). Index $t = 0(1)$ denotes isoscalar(isovector) terms, ρ_{00} is a fixed number. $C_{t0}^{\rho\rho}$, $C_{tD}^{\rho\rho}$, $C_t^{\rho\Delta\rho}$, $C_t^{\rho\tau}$, $C_t^{J^2}$, $C_t^{\rho\nabla J}$, γ , V_0^n , and V_0^p are parameters. Definitions of densities appearing in Eq. (3.6) are listed in Table 3.1 [3].

In Table 3.1, $q = \pm\frac{1}{2}$ is the same as that in Eq. (3.6). $\sigma = \pm\frac{1}{2}$ is the spin projection. $\boldsymbol{\sigma}$ is the spin Pauli matrix. $\rho(\mathbf{r}\sigma q; \mathbf{r}\sigma q)$ and $\kappa(\mathbf{r}\sigma q; \mathbf{r} - \sigma q)$ are the density matrix and pairing tensor, respectively, as defined in Table 2.3.2 in coordinate space. The relation between the parameters in Eq. (3.6) and those in Skyrme force defined by (2.25) can be found in Ref. [53].

Because for the UNEDF0 parametrization $C_{t=0,1}^{J^2}$ are set to 0 [22], in our case the set of parameters that is used for calculating the observables is

$$\mathcal{A} = \left\{ C_{t0}^{\rho\rho}, C_{tD}^{\rho\rho}, C_t^{\rho\Delta\rho}, C_t^{\rho\tau}, C_t^{\rho\nabla J} \right\}_{t=0,1} \cup \{ \gamma, V_0^n, V_0^p \}. \quad (3.8)$$

However, in the fitting process of UNEDF0, the parameter set in use is chosen as

$$\mathcal{B} = \left\{ C_t^{\rho\Delta\rho}, C_t^{\rho\nabla J} \right\}_{t=0,1} \cup \{ \rho_c, E^{\text{NM}}/A, M_s^{*-1}, a_{\text{sym}}^{\text{NM}}, L_{\text{sym}}^{\text{NM}}, K^{\text{NM}}, V_0^n, V_0^p \}, \quad (3.9)$$

where ρ_c is the equilibrium density, $\frac{E^{\text{NM}}}{A}$ is the total energy per nucleon at equilibrium, M_s is the isovector effective mass, $a_{\text{sym}}^{\text{NM}}$ is the symmetry energy coefficient, $L_{\text{sym}}^{\text{NM}}$ is the density

Symbol	Name	Defination
$\rho_0(\mathbf{r})$	iso-scalar density	$\rho_0(\mathbf{r}, \mathbf{r}) = \sum_{\sigma, q} \rho(\mathbf{r}\sigma q; \mathbf{r}\sigma q)$
$\rho_1(\mathbf{r})$	iso-vector density	$\rho_1(\mathbf{r}, \mathbf{r}) = 2 \sum_{\sigma, q} q \rho(\mathbf{r}\sigma q; \mathbf{r}\sigma q)$
$\tilde{\rho}_q(\mathbf{r})$	abnormal density	$\tilde{\rho}_q(\mathbf{r}) = -2 \sum_{\sigma} \sigma \kappa(\mathbf{r}\sigma q; \mathbf{r} - \sigma q)$
$\tau_t(\mathbf{r})$	kinetic density	$\nabla \cdot \nabla' \rho(\mathbf{r}, \mathbf{r}') _{\mathbf{r}=\mathbf{r}'}$
$\mathbb{J}_t(\mathbf{r})$	spin-orbit tensor	$\frac{i}{2} (\nabla' - \nabla) \otimes \mathbf{s}_t(\mathbf{r}, \mathbf{r}') _{\mathbf{r}=\mathbf{r}'}$
$\mathbf{J}_t(\mathbf{r})$	spin-orbit current	$\sum_{ijk} \epsilon_{ijk} \mathbb{J}_{jk} \mathbf{e}_i$
$\mathbf{s}_0(\mathbf{r})$	iso-scalar spin density	$\mathbf{s}(\mathbf{r}, \mathbf{r}) = \sum_{\sigma, q} \rho(\mathbf{r}\sigma q; \mathbf{r}\sigma' q) \boldsymbol{\sigma}_{\sigma'\sigma}$
$\mathbf{s}_1(\mathbf{r})$	iso-vector spin density	$\mathbf{s}_1(\mathbf{r}, \mathbf{r}) = 2 \sum_{\sigma, q} q \rho(\mathbf{r}\sigma q; \mathbf{r}\sigma' q) \boldsymbol{\sigma}_{\sigma'\sigma}$

Table 3.1: Densities used in Even Skyme EDF

dependence of the symmetry energy, and K^{NM} is the nuclear-matter incompressibility [3]. This means the covariance matrix obtained after the fitting process is built on set \mathcal{B} . Therefore, in order to carry on the calculations about uncertainty propagation, one needs to know how to construct set

$$\mathcal{A}' = \{C_{t0}^{\rho\rho}, C_{tD}^{\rho\rho}, C_t^{\rho\tau}, \}_{t=0,1} \cup \{\gamma\} \quad (3.10)$$

from set

$$\mathcal{B}' = \{\rho_c, E^{\text{NM}}/A, M_s^{*-1}, a_{\text{sym}}^{\text{NM}}, L_{\text{sym}}^{\text{NM}}, K^{\text{NM}}\}. \quad (3.11)$$

The expressions of parameters in set \mathcal{B}' through those in set \mathcal{A}' are given in Ref. [22], and read as

$$\begin{aligned} C_{00}^{\rho\rho} &= \frac{1}{3\gamma\rho_c} \left\{ \frac{\hbar^2}{2m} [(2-3\gamma)M_s^{*-1} - 3] \tau_c + 3(1+\gamma) \frac{E^{\text{NM}}}{A} \right\}, \\ C_{0D}^{\rho\rho} &= \frac{1}{3\gamma\rho_c^{1+\gamma}} \left\{ \frac{\hbar^2}{2m} (3-2M_s^{*-1}) \tau_c - 3 \frac{E^{\text{NM}}}{A} \right\}, \\ C_0^{\rho\tau} &= \frac{\hbar^2}{2m} (M_s^{*-1} - 1) \frac{1}{\rho_c}, \\ C_1^{\rho\tau} &= C_0^{\rho\tau} - \frac{\hbar^2}{2m} (M_v^{*-1} - 1) \frac{1}{\rho_c} \quad (3.12) \\ C_{10}^{\rho\rho} &= \frac{1}{27\gamma\rho_c} \left[27(1+\gamma) a_{\text{sym}}^{\text{NM}} - 9L_{\text{sym}}^{\text{NM}} + 5\tau_c(2-3\gamma)(C_0^{\rho\tau} + 3C_1^{\rho\tau}) \rho_c - 5\tau_c(1+3\gamma) \frac{\hbar^2}{2m} \right], \\ C_{1D}^{\rho\rho} &= \frac{1}{27\gamma\rho_c^{1+\gamma}} \left\{ -27a_{\text{sym}}^{\text{NM}} + 9L_{\text{sym}}^{\text{NM}} + 5 \left[\frac{\hbar^2}{2m} - 2\rho_c(C_0^{\rho\tau} + 3C_1^{\rho\tau}) \right] \tau_c \right\}, \\ \gamma &= \frac{\frac{\hbar^2}{2m} (4M_s^{*-1} - 3) \tau_c - K^{\text{NM}} - 9 \frac{E^{\text{NM}}}{A}}{\frac{\hbar^2}{2m} (6M_s^{*-1} - 9) \tau_c + 9 \frac{E^{\text{NM}}}{A}}. \end{aligned}$$

In the formula above, $\tau_c = \frac{3}{5} \left(\frac{3\pi^2}{2} \right)^{2/3} \rho_c^{2/3}$, and M_v^{*-1} is the isovector effective mass, which is fixed to a constant in the case of UNEDF0.

Chapter 4

The Lipkin method

From the description in Chapter 2, one sees that the projection methods can improve the mean-field results. By using these methods, one can restore the symmetries in the symmetry-unrestricted wave functions and thus include part of the dynamic correlations. However, the projection methods, especially the VAP method, is highly computationally expensive. To overcome this problem, one can develop approximate methods. The Lipkin method discussed in article II, as I shall show in this chapter, is an approximate method of obtaining the VAP results. In this chapter, I review the general idea of the Lipkin method represented in Sec. II of article II. Supplementary materials that are useful in practical calculations are also given in this chapter.

4.1 General concepts of the Lipkin method

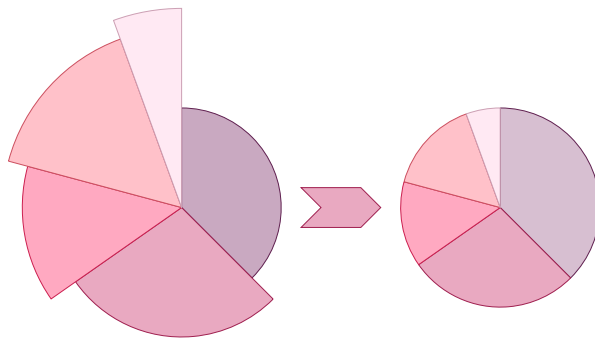


Figure 4.1: A schematic diagram of the Lipkin method. Each sector represents a good-quantum-number component in the ground state corresponding to the symmetry one wants to restore. Its radius is the average energy of the component. Its angle is the weight of the component in the ground state. In the left panel, different components have different energies and the ground-state energy depends on how they are mixed. In the right panel, the energy differences between different components are flattened by the Lipkin method. The ground-state energy becomes independent of how the components are mixed.

As pointed out in Sec. I of article II, the Lipkin method (LM) can be viewed as an approximation of the VAP method. To restore a given quantum number with this method, one tries to add

suitable terms to the Hamiltonian to form a Routhian so that all components with different target quantum numbers in the symmetry-broken ground state give the same expectation value of this Routhian [54, 55]. In this way, the projected energy can be calculated without any projection.

To demonstrate this, as shown in Sec. II of article II, one can consider a symmetry operator \hat{O} which commutes with \hat{H} . For simplicity, I assume \hat{O} is a one-body operator. The mean-field state $|\Phi\rangle$ can be written as a superposition of orthonormalized eigenstates of \hat{O} :

$$|\Phi\rangle = \sum_i a_i |O_i\rangle. \quad (4.1)$$

The projected energy of the state $|O_i\rangle$ is

$$E_i = \langle O_i | \hat{H} | O_i \rangle. \quad (4.2)$$

If E_i is an analytic function of O_i , one can decompose it into

$$\begin{aligned} E_i &= E_0 + f(O_i), \\ E_0 &= E_i(O_i = 0), \quad f(O_i = 0) = 0, \end{aligned} \quad (4.3)$$

where \hat{O} is assumed to be defined in such a way that it has 0 eigenvalue, and E_i is supposed to reach its minimum at $i = 0$. By using this decomposition, the energy of the ground state $|\Phi\rangle$ becomes

$$\begin{aligned} E &= \frac{\langle \Phi | \hat{H} | \Phi \rangle}{\langle \Phi | \Phi \rangle} = \frac{\sum_i |a_i|^2 E_i}{\sum_i |a_i|^2} \\ &= E_0 + \frac{\sum_i |a_i|^2 f(O_i)}{\sum_i |a_i|^2} = E_0 + \frac{\langle \Phi | f(\hat{O}) | \Phi \rangle}{\langle \Phi | \Phi \rangle}. \end{aligned} \quad (4.4)$$

Thus, E_0 is given by

$$E_0 = \frac{\langle \Phi | \hat{H} - f(\hat{O}) | \Phi \rangle}{\langle \Phi | \Phi \rangle}. \quad (4.5)$$

This means that the mean-field ground state, which is obtained by applying the variational principle to the Routhian $\hat{H} - f(\hat{O})$ can give us the projected energy of the ground state $|O_i = 0\rangle$. Thus, the Lipkin method can be viewed as an approximation of the VAP method. Of course, the mean-field ground states obtained in this way are not eigenstates of the symmetry operator. One still need to use projection methods to restore their symmetries.

4.2 Determination of $f(\hat{O})$

4.2.1 The Taylor expansion

In order to use the Lipkin method, one should determine the Lipkin operator $f(\hat{O})$ first. A practical way to do this is to expand $f(O_i)$ up to order N :

$$f(O_i) = \sum_{n=1}^N k_n O_i^n. \quad (4.6)$$

Then the problem becomes how to determine the coefficients in Eq. (4.6). To calculate k_n , one can define a state

$$|\Phi(r)\rangle = \hat{S}(r)|\Phi\rangle, \quad \hat{S}(r) = \exp[-i\hat{Q}r]. \quad (4.7)$$

where r is a real parameter and \hat{Q} is a Hermitian generator of the symmetry \hat{O} , which commutes with both \hat{H} and \hat{O} . The expectation value of \hat{H} between $|\Phi\rangle$ and $|\Phi(r)\rangle$ is

$$\begin{aligned} \langle\Phi|\hat{H}|\Phi(r)\rangle &= \sum_{ij} a_i a_j^* \langle O_i | \hat{H} e^{-i\hat{Q}r} | O_j \rangle \\ &= \sum_i |a_i|^2 E_i \langle O_i | e^{-i\hat{Q}r} | O_i \rangle. \end{aligned} \quad (4.8)$$

In the last line, $1 = \sum_k |O_k\rangle\langle O_k|$ is used.

Inserting Eqs. (4.3) and (4.6) into (4.8), one gets

$$\begin{aligned} \langle\Phi|\hat{H}|\Phi(r)\rangle &= E_0 \sum_i |a_i|^2 \langle O_i | e^{-i\hat{Q}r} | O_i \rangle + \sum_n k_n \sum_i |a_i|^2 O_i^n \langle O_i | e^{-i\hat{Q}r} | O_i \rangle \\ &= E_0 \langle\Phi|\Phi(r)\rangle + \sum_{n=1}^N k_n \langle\Phi|\hat{O}^n|\Phi(r)\rangle, \end{aligned} \quad (4.9)$$

where the fact that \hat{Q} and \hat{O} commute is used.

From Eq. (4.9), one can construct linear equations of k_n by taking $n+1$ different r values r_0, r_1, \dots, r_n provided the dependence of the kernel $\langle\Phi|\hat{O}^n|\Phi(r)\rangle$ on r is known, that is,

$$\begin{aligned} \mathcal{A}\mathbf{k} &= \mathbf{h}, \\ \mathcal{A}_{ij} &= \frac{\langle\Phi|\hat{O}^j|\Phi(r_i)\rangle}{\langle\Phi|\Phi(r_i)\rangle}, \\ h_i &= \frac{\langle\Phi|\hat{H}|\Phi(r_i)\rangle}{\langle\Phi|\Phi(r_i)\rangle}, \\ k_0 &= E_0. \end{aligned} \quad (4.10)$$

In the above, one actually assumes that \hat{O} is a scalar. If $\hat{O} = (O^{(1)}, \dots, O^{(l)})$ is a vector, and the eigenstate can be labeled as $|O_i\rangle = |O_i^{(1)} \dots O_i^{(l)}\rangle$, Eq. (4.6) becomes

$$f(O_i) = \sum_{m=1}^l k_m^{(1)} O_i^{(m)} + \sum_{m,n=1}^l k_{mn}^{(2)} O_i^{(m)} O_i^{(n)} + \dots \quad (4.11)$$

One may still use Eq. (4.10) to determine coefficients in the expansion. But now terms like

$$\mathcal{A}_{(mn)j} = \frac{\langle\Phi|\hat{O}^{(m)}\hat{O}^{(n)}|\Phi(r_i)\rangle}{\langle\Phi|\Phi(r_i)\rangle} \quad (4.12)$$

appear.

4.2.2 The expression for \mathcal{A}

One sees that to calculate the matrix element of \mathcal{A} is the same as to calculate the reduced kernel of a product of n one-body operators between two states $|\Phi\rangle$ and $|\Phi(r)\rangle$. The product can be written as

$$\begin{aligned} \mathcal{S}_n &= \hat{A}_n \hat{A}_{n-1} \cdots \hat{A}_2 \hat{A}_1, \\ \hat{A}_l &= \sum_{ij} A_{l;mn} c_i^\dagger c_j, \quad l = 1, 2, \dots, n. \end{aligned} \quad (4.13)$$

If $|\Phi(r)\rangle$ has the same number parity [18] as $|\Phi\rangle$ (they both only have even particle-number components, or both only have odd particle-number components), then $S_n \equiv \frac{\langle \Phi | \mathcal{S}_n | \Phi(r) \rangle}{\langle \Phi | \Phi(r) \rangle}$ can be calculated from the following recurrence relation:

$$\begin{aligned} S_{l+1} &= \text{Tr} [A_{l+1} \rho_r] S_l \\ &\quad + \text{Tr} [A_{l+1} (1 - \rho_r) S_l^\rho \rho_r] - \text{Tr} \left[\left(A_{l+1} \kappa_r' \right)^* S_l^\rho \kappa_r \right] \\ &\quad - \text{Tr} [A_{l+1} \kappa_r S_l^\kappa \rho_r] + \text{Tr} \left[A_{l+1} (1 - \rho_r) S_l^{\kappa c} \kappa_r' \right], \\ S_1 &= \text{Tr} [A_1 \rho_r], \quad l = 0, 1, \dots, n-1, \\ S_{l;ij}^\rho &\equiv \frac{\partial S_l}{\partial \rho_{r;ji}}, \quad S_{l;ij}^\kappa \equiv \frac{\partial S_l}{\partial \kappa_{r;ji}}, \quad S_{l;ij}^{\kappa c} \equiv \frac{\partial S_l}{\partial \kappa_{r;ji}'}, \end{aligned} \quad (4.14)$$

where ρ_r is the transition density matrix, and κ_r and κ_r' are the transition pairing tensors defined as

$$\begin{aligned} \rho_{r;ij} &= \frac{\langle \Phi | c_j^\dagger c_i | \Phi(r) \rangle}{\langle \Phi | \Phi(r) \rangle}, \\ \kappa_{r;ij} &= \frac{\langle \Phi | c_j c_i | \Phi(r) \rangle}{\langle \Phi | \Phi(r) \rangle}, \quad \kappa_{r;ij}' = \frac{\langle \Phi | c_i^\dagger c_j^\dagger | \Phi(r) \rangle}{\langle \Phi | \Phi(r) \rangle}. \end{aligned} \quad (4.15)$$

When calculating $S_{l;ij}^\rho$, $S_{l;ij}^\kappa$, and $S_{l;ij}^{\kappa c}$, $\rho_{r;ji}$, $\kappa_{r;j>i}$, and $\kappa_{r;j>i}'$ should be treated as independent variables. The derivation of Eq. (4.14) is given in the appendix. See also the analogous derivation presented for the particle-number symmetry in Ref. [56].

4.2.3 Transition density

From Eq. (4.14), one sees that the expressions for the transition density and transition pairing tensor are needed to finish the calculation of \mathcal{A} . They are also needed when calculating h_i . If $|\Phi\rangle$ and $|\Phi(r)\rangle$ are treated as the vacua with respect to quasiparticle operators β and γ , then the corresponding Bogoliulov transformations can be written as

$$\begin{bmatrix} \beta \\ \beta^\dagger \end{bmatrix} = \begin{bmatrix} A_0^\dagger & B_0^\dagger \\ B_0^T & A_0^T \end{bmatrix} \begin{bmatrix} \hat{c} \\ \hat{c}^\dagger \end{bmatrix}, \quad \begin{bmatrix} \hat{\gamma} \\ \hat{\gamma}^\dagger \end{bmatrix} = \begin{bmatrix} A_1^\dagger & B_1^\dagger \\ B_1^T & A_1^T \end{bmatrix} \begin{bmatrix} \hat{c} \\ \hat{c}^\dagger \end{bmatrix}. \quad (4.16)$$

By using the Thouless theorem [57], one can show that

$$\begin{aligned}\rho_r &= B_1^* (A_0^T A_1^* + B_0^T B_1^*)^{-1} B_0^T \equiv \tilde{B}_1^* B_0^T, \\ \kappa_r &= B_1^* (A_0^T A_1^* + B_0^T B_1^*)^{-1} A_0^T \equiv \tilde{B}_1^* A_0^T, \\ \kappa_r' &= B_0^* (A_1^T A_0^* + B_1^T B_0^*)^{-1} A_1^T \equiv B_0^* \tilde{A}_1^T, \\ \tilde{B}_1 &= B_1 (A_0^\dagger A_1 + B_0^\dagger B_1)^{-1}, \\ \tilde{A}_1 &= A_1 (A_0^\dagger A_1 + B_0^\dagger B_1)^{-1},\end{aligned}$$

where A_0^* and B_0^* can be found by solving the mean-field equations.

For A_1^* and B_1^* , because $|\Phi(r)\rangle$ is defined through Eq. (4.7), there should be

$$\begin{aligned}\begin{bmatrix} \gamma \\ \gamma^\dagger \end{bmatrix} &= \begin{bmatrix} A_0^\dagger & B_0^\dagger \\ B_0^T & A_0^T \end{bmatrix} \hat{R} \begin{bmatrix} \hat{c} \\ \hat{c}^\dagger \end{bmatrix} \hat{R}^\dagger, \\ \hat{R} &\equiv \exp[-i\hat{Q}r].\end{aligned}\tag{4.17}$$

The transformation behavior of the creation and annihilation operators under \hat{R} are

$$\begin{aligned}\hat{c}_i^\dagger &\rightarrow \hat{R} \hat{c}_i^\dagger \hat{R}^\dagger = R_{ij}^T \hat{c}_j^\dagger \\ \hat{c}_i = (\hat{c}_i^\dagger)^\dagger &\rightarrow (\hat{R} \hat{c}_i \hat{R}^\dagger)^\dagger = R_{ij}^\dagger \hat{c}_j.\end{aligned}$$

This leads to

$$\begin{bmatrix} \gamma \\ \gamma^\dagger \end{bmatrix} = \begin{bmatrix} A_0^\dagger & B_0^\dagger \\ B_0^T & A_0^T \end{bmatrix} \begin{bmatrix} R^\dagger & 0 \\ 0 & R^T \end{bmatrix} \begin{bmatrix} \hat{c} \\ \hat{c}^\dagger \end{bmatrix}.\tag{4.18}$$

Thus there should be:

$$A_1^* = R^* A_0^* \quad , \quad B_1^* = R B_0^*.$$

If one wants to calculate the abnormal density defined in Table 3.1, it is convenient to build A_0^\dagger and A_1^\dagger on the time-reversed basis. This is because a single-fermion state $|\sigma\rangle$ can be viewed, up to a phase factor, as the time reversal of the state $|\sigma\rangle$, where σ is the spin value. If the operator \hat{R} has the property

$$\hat{R} = \hat{T}^{-1} \hat{R} \hat{T},\tag{4.19}$$

the transformation matrix built on time-reversed basis satisfies the relation

$$\begin{aligned}R_{\bar{a}\bar{b}} &= \langle a | \hat{T}^\dagger \hat{R} \hat{T} | b \rangle \\ &= \langle a | \hat{T}^\dagger \hat{T} (\hat{T}^{-1} \hat{R} \hat{T}) | b \rangle = \langle b | \hat{T}^\dagger | a \rangle \\ &= R_{ab}^*.\end{aligned}\tag{4.20}$$

Therefore, assuming the A^* matrices built on time-reversed basis are $A_{t,0}^*$ and $A_{t,1}^*$, there should be

$$A_{t,1}^* = R A_{t,0}^*,\tag{4.21}$$

which is the same as the relation between B_0^* and B_1^* .

4.2.4 The Gaussian overlap approximation

The Gaussian overlap approximation (GOA) provides us with a fast way to calculate \mathcal{A}_{ij} (Eq. (4.10)) [2, 15]. In Eq. (4.7), in the case of $\hat{Q} = \hat{O}$, one obtains

$$\begin{aligned} \frac{\langle \Phi | \hat{O}^n | \Phi(r) \rangle}{\langle \Phi | \Phi(r) \rangle} &= (-i)^n \mathcal{N}^{-1}(r) \frac{\partial}{\partial r^n} \mathcal{N}(r), \\ \mathcal{N}(r) &\equiv \langle \Phi | \Phi(r) \rangle. \end{aligned} \quad (4.22)$$

The GOA assumes that the kernel $\mathcal{N}(r)$ can be approximated (up to a phase factor) by

$$\mathcal{N}(r) \approx \mathcal{N}_{\text{GOA}}(r) = e^{ir\langle O \rangle} \exp \left[-\frac{r^2}{2} \left(\langle O^2 \rangle - \langle O \rangle^2 \right) \right]. \quad (4.23)$$

If there is $\langle O \rangle = 0$ (this is true when the wave function has time-reversal symmetry and \hat{O} is among those that will be given in Sec. 4.3.1), Eq. (4.23) can be simplified to

$$\mathcal{N}_{\text{GOA}}(r) = e^{-\frac{1}{2}ar^2}, a \equiv \langle \hat{O}^2 \rangle. \quad (4.24)$$

Inserting Eq. (4.24) into Eq. (4.22) gives:

$$\begin{aligned} \frac{\langle \Phi | \hat{O}^n e^{i\hat{O}r} | \Phi \rangle}{\langle \Phi | e^{i\hat{O}r} | \Phi \rangle} &\approx (-i)^n e^{\frac{1}{2}ar^2} \frac{\partial^n}{\partial r^n} e^{-\frac{1}{2}ar^2} \\ &= (-i\sqrt{\frac{a}{2}})^n H_n \left(\sqrt{\frac{a}{2}} r \right), \end{aligned} \quad (4.25)$$

where H_n is the Hermite polynomial of order n .

To use Eq. (4.25), one needs to know the value of a . Eq. (4.24) shows that a can be obtained from the kernel $\mathcal{N}(r)$:

$$a = -\frac{2 \ln \mathcal{N}_{\text{GOA}}(r)}{r^2} \approx -\frac{2 \ln \mathcal{N}(r)}{r^2}. \quad (4.26)$$

Eq. (4.26) becomes exact at the limit $r \rightarrow 0$. To calculate the kernel, one can use the Onishi formula [58]:

$$\mathcal{N}(r) = \sqrt{\det \left(A_1^\dagger A_0 + B_1^\dagger B_0 \right)} = \exp \left\{ \frac{1}{2} \text{Tr} \left[\ln \left(A_1^\dagger A_0 + B_1^\dagger B_0 \right) \right] \right\}. \quad (4.27)$$

But it can't always give the correct phase factor when the pairing is non-zero. An alternative formula that can give the correct phase factor is [59]:

$$\mathcal{N}(r) = \frac{\text{Pf} \begin{bmatrix} B_0^T A_0 & B_0^T B_1^* \\ -B_1^\dagger B_0 & A_0^\dagger B_0^* \end{bmatrix}}{\text{Pf} \begin{bmatrix} B_0^T A_0 & B_0^T B_0^* \\ -B_0^\dagger B_0 & A_0^\dagger B_0^* \end{bmatrix}}, \quad (4.28)$$

where Pf is the Pfaffian of a skew matrix. To use Eq. (4.28), all columns corresponding to pure hole orbits in B_0 and A_0 should be dropped to remove the 0 factor appeared both in the numerator and denominator. Although Eq. (4.28) is only suitable for the kernels defined in Eq. (4.22) with $|\Phi\rangle$ being a ground state of an even-even nucleus, it can be easily generalized to kernels between arbitrary states. See Ref. [59].

4.3 The Lipkin method for the translational- and rotational-symmetry restoration

4.3.1 \hat{O} , \hat{Q} and the Lipkin operator

The choice of \hat{O} and \hat{Q} depends on the specific symmetry one wants to restore. So does the choice of terms included in the Lipkin operator $f(\hat{O})$. As explained in Sec. II of article II, for the translational-symmetry restoration, our choice is

$$f(\hat{\mathbf{P}}) = \sum_{i=x,y,z} k_i \hat{P}_i^2, \quad \hat{Q}_i = \hat{P}_i, \quad r = r_x, r_y, r_z, \quad (4.29)$$

where \hat{P}_i is the total momentum operator in the x -, y - or z -direction. Since now the operator \hat{S} defined in Eq. (4.7) is just the space-shift operator, r_x , r_y and r_z are the corresponding shifting distances. For calculations in article II, the reduced kernel of the square of the total momentum in j direction between the original state $|\Phi\rangle$ and shifted state $\exp[-i\hat{P}_j r_j] |\Phi\rangle$,

$$p_{2,j}(r_i) = \frac{\langle \Phi | \hat{P}_j^2 \exp[-i\hat{P}_j r_j] | \Phi \rangle}{\langle \Phi | \exp[-i\hat{P}_j r_j] | \Phi \rangle}, \quad (4.30)$$

is almost a constant function of r_i when $i \neq j$. A simple proof based on the GOA and symmetry requirements on the mean-field state is given in the appendix. Thus, if only a single \hat{P}_i is used as \hat{Q} , the term $p_{2,j \neq i}(r_i)$ is absorbed into the constant k_0 in Eq. (4.10), which means that one can not determine $k_{j \neq i}$. To guarantee that one can construct enough amount of linear equations that determine k_i , three different \hat{Q} s instead of one should be used. In addition, it is easy to show that this property reduces Eq. (4.10) into three independent equations

$$\begin{bmatrix} h(0) \\ h(r_i) \end{bmatrix} = \begin{bmatrix} 1 & p_2(0) \\ 1 & p_2(r_i) \end{bmatrix} \begin{bmatrix} k_{0,i} \\ k_i \end{bmatrix}, \quad i = x, y, z, \quad (4.31)$$

where

$$p_2(r_i) = \sum_{j=x,y,z} p_{2,j}(r_i),$$

$$k_{0,i} = E_0 + \sum_{j \neq i} (k_j - k_i) p_{2,j}(0),$$

and E_0 is defined in Eq.(4.3).

For the rotational symmetry restoration, we choose

$$f(\hat{\mathbf{J}}^2) = k \hat{\mathbf{J}}^2, \quad \hat{Q} = \hat{J}_y, \quad r = \beta, \quad (4.32)$$

where \hat{J}^2 is the square of the total angular momentum operator, \hat{J}_y is the angular momentum operator in the y direction, and β is the rotation angle around the y -axis. Since in article II we focus on the ground states of axially deformed nuclei, the condition $\langle \hat{J}_z^2 \rangle = 0$ can be satisfied during the variational process. Therefore, $\hat{\mathbf{J}}^2$ can be replaced by $\hat{J}_x^2 + \hat{J}_y^2$.

4.3.2 Symmetries in $f(\hat{O})$

Consider the time reversal first. From Sec. 4.3.1, one sees that for the translational-symmetry restoration, the Lipkin operator has the form $f(\hat{\mathbf{P}}) = \sum_{i=x,y,z} k_i \hat{P}_i^2$. Since \hat{P}_i is the total momentum operator in the i -direction, we have

$$\hat{T}^{-1} \hat{P}_i \hat{T} = -\hat{P}_i. \quad (4.33)$$

This means that \hat{P}_i^2 and thus $f(\hat{\mathbf{P}})$ are invariant under the time-reversal transformation. From a similar discussion, one finds that the Lipkin operator $f(\hat{\mathbf{J}}^2)$ used in the rotational-symmetry restoration is also invariant under the time-reversal transformation.

Then consider an arbitrary unitary symmetry group element \hat{S} . \hat{S} transforms \hat{P}_i^2 into

$$\begin{aligned} \hat{S}^\dagger \hat{P}_i^2 \hat{S} &= \left(\hat{S}^\dagger \hat{P}_i \hat{S} \right)^2 = \left[\sum_{ab} p_{i,ab} \hat{S}^\dagger c_a^\dagger \hat{S} \hat{S}^\dagger c_b \hat{S} \right]^2 \\ &= \left[\sum_{ab} p_{i,ab} \left(\sum_m S_{ma}^\dagger c_m^\dagger \right) \left(\sum_n S_{nb}^T c_n \right) \right]^2 \\ &= \left[\sum_{mn} \langle m | \hat{S}^\dagger \hat{p}_i \hat{S} | n \rangle c_m^\dagger c_n \right]^2. \end{aligned} \quad (4.34)$$

One sees that if

$$\hat{S}^\dagger \hat{p}_i \hat{S} = \pm \hat{p}_i, \quad (4.35)$$

then there is $\hat{S}^\dagger f(\hat{\mathbf{P}}) \hat{S} = f(\hat{\mathbf{P}})$. The same conclusion also holds for $f(\hat{\mathbf{J}}^2)$.

4.3.3 Matrix elements of $f(\hat{O})$

To implement the LM calculation, besides determining the coefficients appearing in the Lipkin operator, one also needs to calculate the matrix elements introduced into the mean-field equation by this operator. In the cases considered in article II, this question can be simplified by calculating the matrix element of $k\hat{O}^2$, where \hat{O}^2 is the square of a one-body operator. By using Eq. (4.14), the expectation value of \hat{O}^2 is

$$\frac{\langle \Phi | \hat{O}^2 | \Phi \rangle}{\langle \Phi | \Phi \rangle} = [\text{Tr}(O\rho)]^2 + \text{Tr}(O^2\rho) - \text{Tr}(O\rho O\rho) - \text{Tr}[O\kappa(O\kappa)^*]. \quad (4.36)$$

From the variational principle, one gets the following matrix elements:

$$\begin{aligned} \frac{\partial}{\partial \rho_{ji}} [\text{Tr}(O\rho)]^2 &= 2\text{Tr}(O\rho) O_{ij} = 2\langle \hat{O} \rangle O_{ij}, \\ \frac{\partial}{\partial \rho_{ji}} \text{Tr}(O^2\rho) &= O_{ij}^2, \\ \frac{\partial}{\partial \rho_{ji}} \text{Tr}(O\rho O\rho) &= \sum_{kl} O_{lj} O_{ik} \rho_{kl} + (O\rho O)_{ij} = 2(O\rho O)_{ij}, \\ \frac{\partial}{\partial \kappa_{ij}^*} \text{Tr}(O\kappa O^* \kappa^*) &= (O\kappa O^T)_{ji} - (O\kappa O^T)_{ij} = -2(O\kappa O^T)_{ij}. \end{aligned} \quad (4.37)$$

From these matrix elements, one can build the matrix which should be added to the \mathcal{H} in Table 2.3.2 after being multiplied with the coefficient $-k$:

$$\begin{aligned}\mathcal{O}_2 &= \begin{bmatrix} O_h & O_\Delta \\ -O_\Delta^* & -O_h^* \end{bmatrix}, \\ O_h &= 2\langle \hat{O} \rangle O + O^2 - 2O\rho O, \\ O_\Delta &= 2O\kappa O^T.\end{aligned}\tag{4.38}$$

Since the operator \hat{O} that we use in article II does not mix protons and neutrons wave functions, and neither we allow proton-neutron mixing during the calculation, the O , ρ and κ matrices only have diagonal blocks:

$$O = \begin{bmatrix} O_n & 0 \\ 0 & O_p \end{bmatrix}, \quad \rho = \begin{bmatrix} \rho_n & 0 \\ 0 & \rho_p \end{bmatrix}, \quad \kappa = \begin{bmatrix} \kappa_n & 0 \\ 0 & \kappa_p \end{bmatrix}.\tag{4.39}$$

In order to treat protons and neutrons separately, in Eq. (4.37), one can make the following replacement:

$$ij \rightarrow q, ij, \quad q = n, p.\tag{4.40}$$

This is equivalent to replacing O by O_q , ρ by ρ_q , and κ by κ_q , except for the first line in Eq. (4.37). In this term, O_{ij} needs to be replaced by $O_{q,ij}$, but $\text{Tr}(O\rho)$ should be replaced by $\text{Tr}(O_p\rho_p) + \text{Tr}(O_n\rho_n)$, since it is a coefficient rather than a matrix element. The matrix \mathcal{O}_2 now becomes

$$\begin{aligned}\mathcal{O}_2 &= \begin{bmatrix} \mathcal{O}_{2,n} & 0 \\ 0 & \mathcal{O}_{2,p} \end{bmatrix}, \\ \mathcal{O}_{2,q} &= \begin{bmatrix} O_{q,h} & O_{q,\Delta} \\ -O_{q,\Delta}^* & -O_{q,h}^* \end{bmatrix}, \\ O_{qh} &= 2\langle \hat{O}_n + \hat{O}_p \rangle O_q + O_q^2 - 2O_q\rho_q O_q, \\ O_{q\Delta} &= 2O_q\kappa_q O_q^T, \quad q = n, p.\end{aligned}\tag{4.41}$$

4.3.4 Other approximate projection methods

Some of the most widely used methods in the rotational-symmetry, translational-symmetry and particle-number restoration are listed in Table 4.1 [60–62].

In Table 4.1, $\hat{\mathbf{J}}$ is the total angular momentum operator. \mathcal{I} is the moment of inertial (MOI). It can be chosen as a mixture of the rigid body and cranking MOIs. $\hat{\mathbf{P}}$ is the total momentum operator, m is the nucleon mass, and A is the particle number. The kinetic term is the term $\sum_{ij} t_{ij}\rho_{ji}$ in Eq. (2.19). The second method for the translational-symmetry restoration is commonly used in the Skyrme-EDF calculation. It is a result of adding the term $-\frac{\hbar^2}{2mA}\langle \sum_k \hat{\mathbf{p}}_k^2 \rangle$, which is the diagonal part of $\frac{\hbar^2}{2mA}\langle \hat{\mathbf{P}}^2 \rangle$, to the EDF. $\hat{\mathbf{p}}_k$ is the momentum of the k^{th} nucleon.

Symmetry	Method
Rotation	$E \rightarrow E - \frac{\hbar^2}{2I} \langle \hat{\mathbf{J}}^2 \rangle$ after variation [60].
Translation	1. $E \rightarrow E - \frac{\hbar^2}{2mA} \langle \hat{\mathbf{P}}^2 \rangle$ before or after variation. 2. $1/m \rightarrow (1-m)[1 - (1/A)]$ in the kinetic term before variation [61].
Particle Number	The Lipkin-Nogami method: $E \rightarrow E - k_2 \langle \hat{N} - \langle \hat{N} \rangle \rangle^2$ before variation [62].

Table 4.1: Several approximate methods to restore symmetries

The Lipkin-Nogami method can be viewed as an example of the Lipkin method for the particle-number restoration. In this method, one uses $k_2 \langle \hat{N} - \langle \hat{N} \rangle \rangle^2$ to flatten the particle-number dependence of the projected energy of particle-number-conserving components in the particle-number-symmetry-breaking mean-field state. However, in the Lipkin-Nogami method, to determine the coefficient k_2 one uses diagonal and not transition matrix elements of the particle-number operator.

Chapter 5

Results

In this chapter, I review the main results of articles I and II.

5.1 Uncertainty propagation

In article II, we calculated the uncertainties of several observables in semi-magic nuclei. A more detailed analysis was done for ^{208}Pb .

In Fig. 5.1, the binding energies, two neutron (proton) separation energies, and neutron (proton) rms radii are plotted. A common feature is that all the uncertainties are small in experimentally known region, whereas they increase when moving towards unknown neutron-rich region. This is a result of poorly constrained isovector parameters in the EDF. For the binding energies, in general, the residues with respect to experimental data are larger than the standard errors for many nuclei. This indicates that there are missing pieces in our model. For two neutron (proton) separation energies, the cancellation between uncertainties makes their statistical uncertainties much smaller than those in binding energies. In the last two rows of Fig. 5.1, one can see that because experimental data of proton radii were used in the parameter optimization, the standard errors for proton radii are smaller compared with those of neutron radii. For proton radii, the standard errors also increase when approaching the proton drip line. This can be interpreted by the weak binding of protons in these light nuclei.

In Fig. 5.2, we show the calculated proton and neutron densities in ^{208}Pb . Obviously, the uncertainties of proton densities are much smaller than those of neutrons. For the neutron densities, by comparing with the sum of experimental and model uncertainties, we found that our standard errors are already much smaller. Therefore, any inclusion of small corrections should not change our results significantly.

In Fig. 5.3, we illustrate the contributions of different terms in Eq. (3.1). One can see that although some diagonal terms may give quite large positive contributions, it is canceled by the negative contributions of the same order from their neighboring off-diagonal terms.

Besides these quantities, the theoretical uncertainties of the single-particle energies, which are not strictly speaking observables are also surveyed. The fact that we obtained small uncertainties shows that the single-particle energies are already tightly constrained by the model. It is unlikely to improve them merely by refitting the parameters of the standard Skyrme EDF.

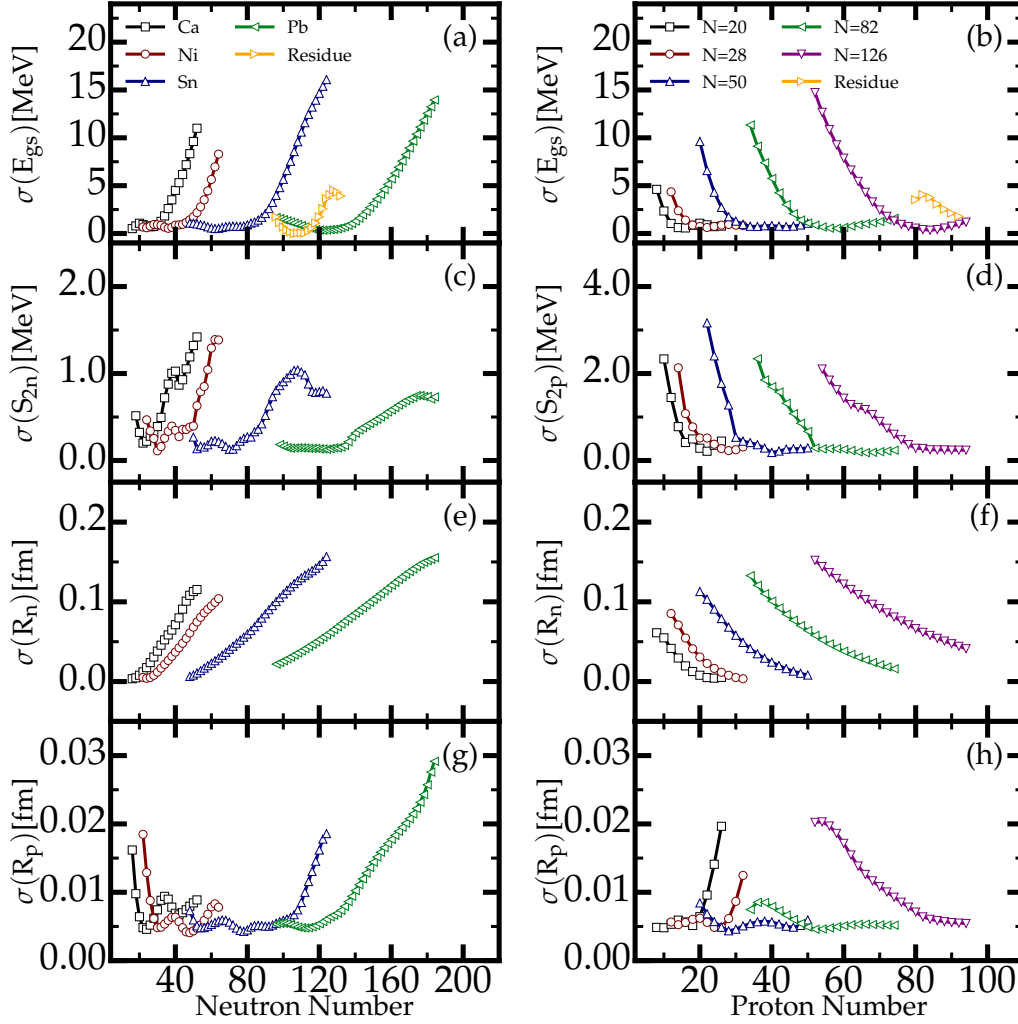


Figure 5.1: Propagated uncertainties of binding energies, two neutron(proton) separation energies, neutron rms radii, and proton rms radii for (a), (c), (e), (g) isotonic chains with magic neutron numbers and (b), (d), (f), (h) isotopic chains with magic proton numbers. For the binding energies of Pb and N = 126 nuclei, fit residuals with respect to experimental data are also shown. Replotted from Fig. 1 to Fig. 4 in article I.

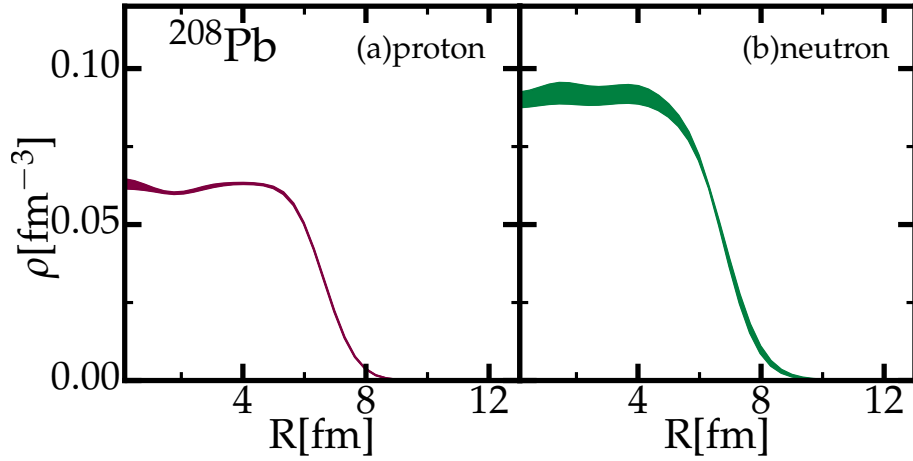


Figure 5.2: Propagated uncertainties of proton (neutron) densities as functions of the radial position in ^{208}Pb . Replotted from Fig. 5 in article I.

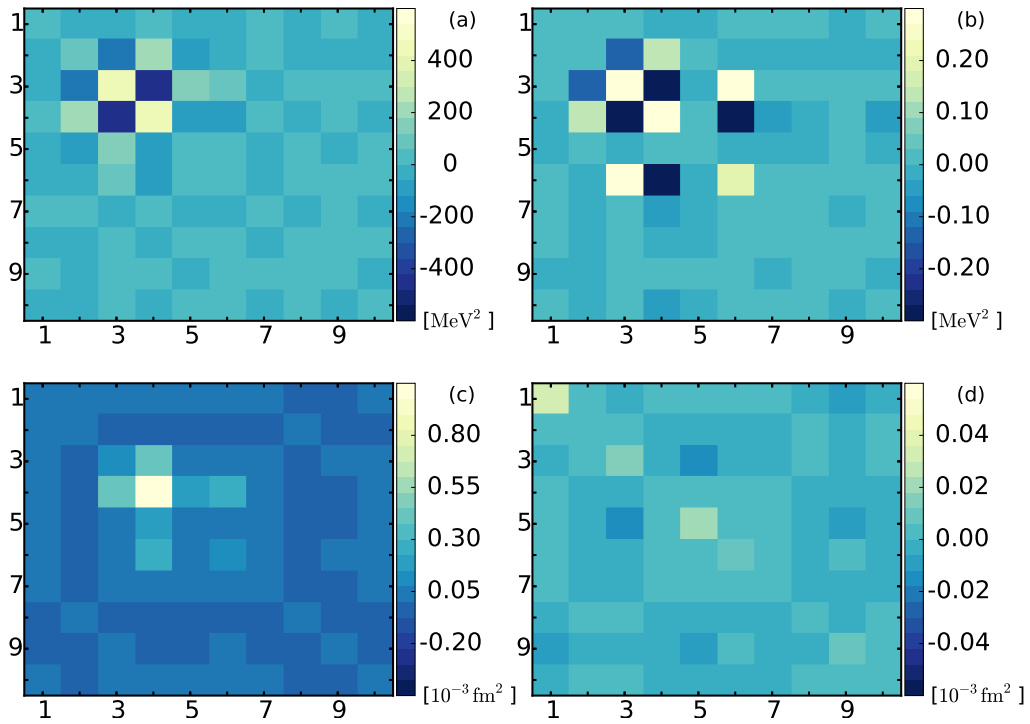


Figure 5.3: Contributions of each term in Eq. (3.1) to squares of standard errors of (a) binding energy, (b) two-neutron separation energy, (c) neutron rms radius, and (d) proton rms radius in ^{208}Pb . The numbers 1 ~ 10 represent ρ_c , E^{NM}/A , $a_{\text{sym}}^{\text{NM}}$, $L_{\text{sym}}^{\text{NM}}$, $C_0^{\rho\Delta\rho}$, $C_1^{\rho\Delta\rho}$, V_0^n , V_1^n , $C_0^{\rho\Delta J}$, and $C_1^{\rho\Delta J}$ as defined in article I. Replotted from Fig. 6 in article I.

5.2 Symmetry restoration with the Lipkin method

In article II, we applied the Lipkin method to the translational-symmetry restoration to the isotopes of elements between proton number $Z = 50$ and $Z = 82$ (the rare-earth-element region) and rotational-symmetry restoration to deformed Er isotopes. For the translational-symmetry restoration, in Fig. 5.4, we plot the ratios between the averaged Lipkin masses (M_{LM}) in the x and y -directions and the exact masses, the differences between the mass ratios in the x - and y -directions, and the differences between the averaged mass ratios in the x - and y -directions and those in the z -direction. It turns out that the mass ratios in all three directions are near but not equal to 1 ((a) in Fig. 5.4). This is because the Lipkin mass and exact mass are two different things. The exact mass describes the dynamic behavior of a nucleus. It reflects how the nucleus reacts under a shift. The Lipkin mass, on the other hand, is the same as the Peierls-Yoccoz mass [55]. It describes some aspects of the stationary property of a nucleus. The quantity $1/2M_{LM}$ in the i -direction is nothing but the coefficient of P_i^2 (the total momentum in the i -direction) term in the expansion of the energy of each component in the ground state with good total momentum.

To demonstrate this difference, one can consider, in the coordinate space, a model Hamiltonian \hat{H}_M of an A -particle nucleus that can be decomposed into a center-of-mass term and intrinsic term:

$$\hat{H}_M = -\frac{\nabla_{\mathbf{R}}^2}{2mA} + \hat{H}_{\text{intr}}, \quad (5.1)$$

where $-\nabla_{\mathbf{R}}^2$ is the total momentum operator and m is the nucleon mass. Let $|\mathbf{P}\rangle$ be a proper normalized component with good total momentum in $|\Phi\rangle$, which is the mean-field ground state of \hat{H}_M . the wave function of $|\mathbf{P}\rangle$ in the coordinate space can be written as

$$\langle \mathbf{X} | \mathbf{P} \rangle \rightarrow e^{-i\mathbf{P}\cdot\mathbf{R}} \phi_{\text{intrinsic}}^{(\mathbf{P})}(\boldsymbol{\xi}). \quad (5.2)$$

where \mathbf{X} represents the space, spin, and isospin coordinates of all nucleons in the laboratory frame, $\boldsymbol{\xi}$ represents all these coordinates in the intrinsic frame, \mathbf{R} is the space coordinate of the center of mass, and $\phi_{\text{intrinsic}}^{(\mathbf{P})}$ is the intrinsic wave function. In general different $|\mathbf{P}\rangle$ can have different intrinsic wave functions.

From Eqs. (5.1) and (5.2), one finds that the energy of state $|\mathbf{P}\rangle$ is

$$E_{\mathbf{P}} = \frac{\mathbf{P}^2}{2mA} + \int d\boldsymbol{\xi} \phi_{\text{intrinsic}}^{(\mathbf{P})*} \hat{H}_{\text{intr}} \phi_{\text{intrinsic}}^{(\mathbf{P})}. \quad (5.3)$$

Because of the second term in Eq. (5.3), when $E_{\mathbf{P}}$ is expanded as a Taylor series of \mathbf{P} , the coefficients of the second-order terms do not need to be the same as the exact mass.

One can also see that there is almost no difference between the Lipkin masses in the y - and x -directions for most of the nuclei ((b) in Fig. 5.4). This is reasonable because most of the calculated nuclei have axial symmetry with z -axis the symmetry axis. Thus the x - and y -directions are symmetric.

What's more, in some nuclei, there are differences between the Lipkin masses in the x/y -direction and those in the z -direction ((c) in Fig. 5.4). This is caused by the deformation ((d) and (e) in Fig. 5.4). If a nucleus has prolate deformation, its density distribution expands more along the z -axis while shrinking along the x - and y -axes. The momentum distribution, to the contrary,

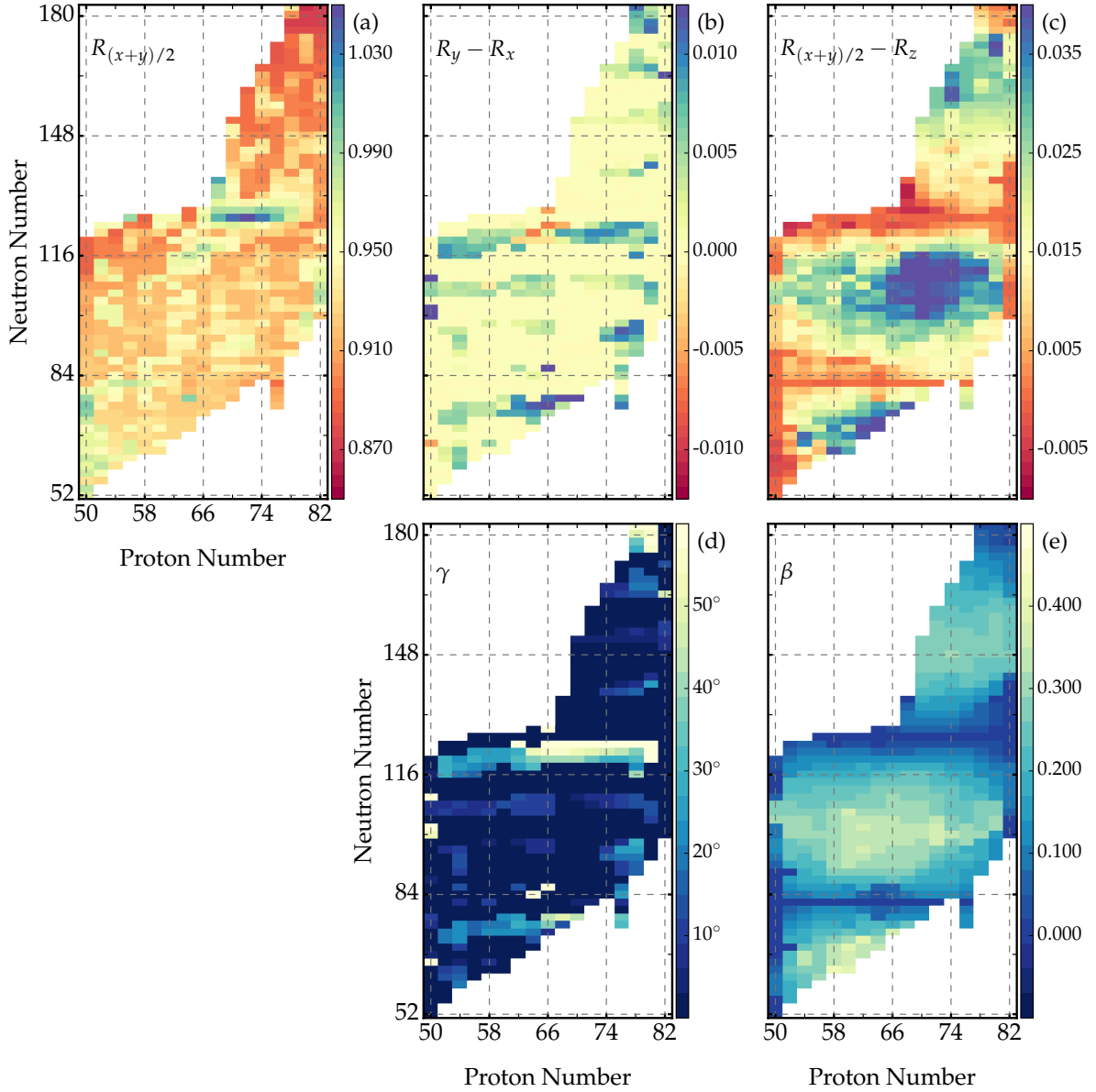


Figure 5.4: (a) $R_{(x+y)/2}$: The ratio between the average of the Lipkin masses in the x and y -directions and the exact mass. (b) $R_y - R_x$: The difference between the mass ratios in the y - and x -directions. (c) $R_{(x+y)/2} - R_z$: The difference between $R_{(x+y)/2}$ and the mass ratio in the z -direction. (d) Gamma deformations. (e) Beta deformations. Replotted from Figs. 2 ~ 4 in article II.

expands more along the x - and y -axes and shrinks along the z -axis. This means that there are relatively more components with relatively large P_x and P_y than components with relatively large P_z . Thus, flatter energy curves and larger Lipkin masses in the x - and y -direction when compared with those in the z -direction become energy preferred.

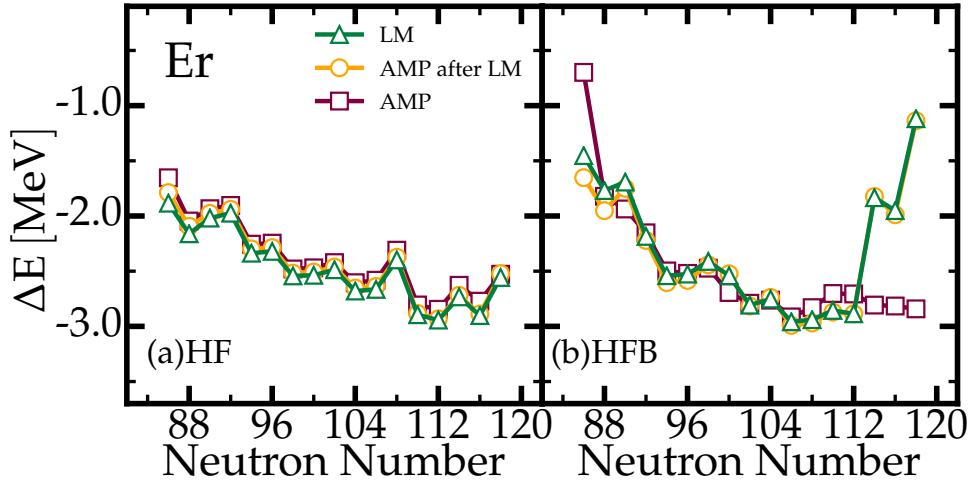


Figure 5.5: Energy corrections from the AMP, Lipkin method and AMP after Lipkin method for Er isotopes with pairing interaction (a) turned off or (b) activated. Replotted from Fig. 6 in article II.

For the rotational-symmetry restoration, in Fig. 5.5, we show the energy corrections for well deformed Er isotopes, namely, $^{86-118}\text{Er}$, that are obtained from the angular momentum projection (AMP) method, Lipkin method and AMP after Lipkin method. Although the SCMF calculations in our case are not the same as Hartree-Fock (HF) or Hartree-Fock-Bogoliubov (HFB) calculations [15] because of the use of the EDF generator, here I still use the term HF (HFB) to represent calculations without (with) pairing. One can see that in general, both for the case with and without pairing, the results given by the Lipkin method are similar with those given by projection either before or after the convergence of the Lipkin method. For $^{182-186}\text{Er}$, the correction energy obtained from AMP are quite different from those in LM or AMP after LM. This is due to the change in nuclei shape after the convergence of the Lipkin method. Despite of these differences, the results indicate that one can use the Lipkin method as an approximation of the VAP method in these Er isotopes.

The moment of inertial (MOI) for well deformed Er isotopes are also calculated with both the cranking and Lipkin method. In Fig. 5.6 one can see that MOIs from these two methods are quite different when the pairing interaction is turned off. If one activates the pairing, the LM MOIs do not change much while the cranking MOIs significantly decrease, so that the values of the latter become much closer to those of the former.

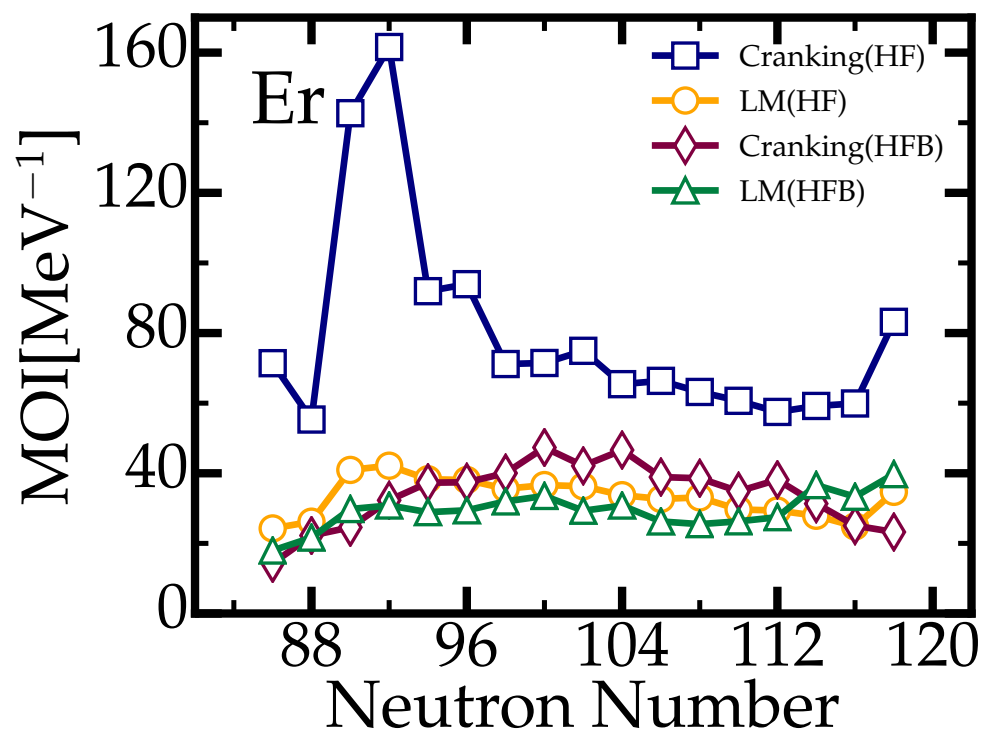


Figure 5.6: MOIs obtained from HF or HFB calculations with the cranking or Lipkin method for Er isotopes. From Fig. 9 in article II.

Chapter 6

Summary

In this thesis, I presented both the theoretical frameworks and numeric results pertaining to the error analysis and Lipkin method. These are the main topics of articles I and II. In addition, I also briefly introduced the DFT theory and SCMF method that provide the theoretical background of the two methods mentioned above.

For the error analysis, I described the formulas describing the uncertainty propagation. Ways to obtain the quantities appearing in these formulas are also given. This analysis is applied to a survey of the effectiveness of the UNEDF0 parameterization in describing semi-magic nuclei. The results show that, because of the poorly constrained isovector parameters, the statistical errors increase towards neutron-rich region. Therefore, the predictive power of the model in this region may be improved if the uncertainties of these parameters are reduced by experimental data. On the other hand, in some cases, the theoretical uncertainties are significantly smaller than the residues between the experimental data and calculated results. This indicates missing terms in the used model, which cannot be absorbed merely by parameter fitting.

For the Lipkin method, I first discussed general procedures to determine the Lipkin operator. Then I focused on using this method to restore the translational and rotational symmetries. The Lipkin operators used in these two cases were determined. I also presented their symmetry properties as well as matrix elements that are introduced into the mean-field equation in this thesis. Numerical calculations related to the translational-symmetry restoration were performed for all even-even isotope chains from proton number $Z = 50$ to $Z = 82$. From the results, one can see that for the translational-symmetry-restoration case, the Lipkin masses and exact masses have similar but nevertheless different values. In deformed nuclei, the Lipkin masses in different directions are different. Calculations concerning the rotational-symmetry restoration were performed for axially deformed erbium isotopes. It was found that the Lipkin method can give similar energy corrections as the AMP of states obtained by applying the Lipkin method. This indicates that the Lipkin method can be treated as a good approximation of the VAP method.

Appendix A

Derivation of the relation (4.14)

Consider a product of n one-body hermitian operators

$$\begin{aligned}
\mathcal{S}_n &= \hat{A}_n \hat{A}_{n-1} \cdots \hat{A}_2 \hat{A}_1 \\
&= \sum_{k_n l_n} \cdots \sum_{k_1 l_1} A_{n; k_n l_n} \cdots A_{n; k_1 l_1} c_{k_n}^\dagger c_{l_n} \cdots c_{k_1}^\dagger c_{l_1} \\
&\equiv \sum_{KL(n)} A_{KL(n)} C_{KL(n)},
\end{aligned} \tag{A.1}$$

where $\sum_{KL(n)} \equiv \sum_{k_n l_n} \cdots \sum_{k_1 l_1}$, $A_{KL(n)} \equiv A_{n; k_n l_n} \cdots A_{n; k_1 l_1}$, $C_{KL(n)} \equiv c_{k_n}^\dagger c_{l_n} \cdots c_{k_1}^\dagger c_{l_1}$. From the Wick theorem, the reduced kernel of \mathcal{S}_n with respect to state $|\Phi\rangle$ can be written as:

$$\begin{aligned}
S_n &\equiv \frac{\langle \Phi | \mathcal{S}_n | \Phi \rangle}{\langle \Phi | \Phi \rangle} = \sum_{KL(n)} A_{KL(n)} W_{KL(n)} \\
&= \sum_{KL(n)} A_{KL(n)} \left(\sum_{\text{all F}} F_{KL(n)} \right),
\end{aligned} \tag{A.2}$$

where $F_{KL(n)}$ is a fully contracted term, and $W_{KL(n)} = \sum_{\text{all F}} F_{KL(n)}$ is the sum of all different fully-contracted terms of $C_{KL(n)}$. The possible contractions between two operators in $F_{KL(n)}$ are

$$\begin{aligned}
\rho_{ij} &\equiv \frac{\langle \Phi | c_j^\dagger c_i | \Phi \rangle}{\langle \Phi | \Phi \rangle}, \quad \rho_{ij}^{\text{iv}} \equiv \frac{\langle \Phi | c_i c_j^\dagger | \Phi \rangle}{\langle \Phi | \Phi \rangle}, \\
\kappa_{ij} &\equiv \frac{\langle \Phi | c_j c_i | \Phi \rangle}{\langle \Phi | \Phi \rangle}, \quad \kappa_{ij}^* \equiv \frac{\langle \Phi | c_i^\dagger c_j^\dagger | \Phi \rangle}{\langle \Phi | \Phi \rangle}.
\end{aligned} \tag{A.3}$$

This means that $F_{KL(n)}$ can be expressed as a product of matrix elements ρ_{ij} , ρ_{ij}^{iv} , κ_{ij} and/or κ_{ij}^* .

Since $C_{KL(n)} = c_{k_n}^\dagger c_{l_n} C_{KL(n-1)}$, the fully contracted terms can be divided into two types:

1. Contract $c_{k_n}^\dagger$ with c_{l_n} ; Fully contract the remaining operator product $C_{KL(n-1)}$:

$$\overbrace{c_{k_n}^\dagger c_{l_n}} C_{KL(n-1)}. \tag{A.4}$$

2. Contract $C_{KL(n-1)}$ until only two operators left; Contract one of the remaining two operators with $c_{k_n}^\dagger$ and the other one with c_{l_n} :

$$c_{k_n}^\dagger \overbrace{c_{l_n}} \overbrace{C_{KL(n)}}. \quad (\text{A.5})$$

For the first type, it is easy to show that its total contribution to S_n is

$$S_{n;1} = \text{Tr} [A_n \rho] S_{n-1}. \quad (\text{A.6})$$

To calculate the total contribution from the second type, we first consider how to find a fully-but-two contracted term with the form

$$T_{KL(n-1)}^{ij} \equiv \cdots c_i^\dagger \cdots c_j \cdots. \quad (\text{A.7})$$

Eq. (A.7) means that $T_{KL(n-1)}^{ij}$ is a fully-but-two contracted term with only c_i^\dagger and c_j left, and c_i^\dagger is at the left of c_j . Since this term will finally contract with $c_{k_n}^\dagger c_{l_n}$, according to the Wick theorem, one can move c_i^\dagger and c_j to the leftmost position and rewrite this term as

$$T_{KL(n-1)}^{ij} = (-)^n c_i^\dagger c_j \cdots, \quad (\text{A.8})$$

where n is the total number of creation and annihilation operators between c_i^\dagger and c_j . On the other hand, one can build a fully contracted term by contracting c_i^\dagger and c_j :

$$F_{KL(n-1)} \equiv \overbrace{T_{KL(n-1)}^{ij}} = \cdots \overbrace{c_i^\dagger \cdots c_j} \cdots. \quad (\text{A.9})$$

The contraction line between c_i^\dagger and c_j contributes a factor $(-1)^n \rho_{ji}$. Thus, by replacing the factor ρ_{ji} in $F_{KL(n-1)}$ with $c_i^\dagger c_j$, one actually obtains

$$\frac{F_{KL(n-1)}}{\rho_{ji}} c_i^\dagger c_j = (-)^n c_i^\dagger c_j \cdots = T_{KL(n-1)}^{ij}. \quad (\text{A.10})$$

Since $F_{KL(n)}$ has the form of a product, from the Libniz formula, if one treats all ρ_{ji} and ρ_{ji}^{iv} as independent variables, the following expression

$$\hat{\mathcal{F}}_{KL(n-1);ij}^\rho = \frac{\partial F_{KL(n-1)}}{\partial \rho_{ji}} c_i^\dagger c_j + \frac{\partial F_{KL(n-1)}}{\partial \rho_{ji}^{\text{iv}}} c_j c_i^\dagger, \quad (\text{A.11})$$

gives the summation of all different $T_{KL(n-1)}^{ij}$ and $T_{KL(n-1)}^{ij,\text{iv}}$ that can be contracted into $F_{KL(n-1)}$. Here

$$T_{KL(n-1)}^{ij,\text{iv}} \equiv \cdots c_j \cdots c_i^\dagger \cdots. \quad (\text{A.12})$$

It is also a fully-but-two contracted term as $T_{KL(n-1)}^{ij}$ except that the order of c_i^\dagger and c_j is inverted. To verify Eq.(A.11), one just needs to notice that here the effect of the operator $\partial/\partial \rho_{ji}$ ($\partial/\partial \rho_{ji}^{\text{iv}}$) is summing up all different terms obtained by removing one ρ_{ji} (ρ_{ji}^{iv}) in $F_{KL(n-1)}$. Once again, because $\hat{\mathcal{F}}_{KL(n-1);ij}^\rho$ will contract with $c_{k_n}^\dagger c_{l_n}$, one can do the replacement $c_j c_i^\dagger \rightarrow -c_j c_i^\dagger$

in Eq. (A.11). Therefore, if one only takes all ρ_{ji} as independent variables, by using the relation $\partial\rho_{ji}/\partial\rho_{ji}^{\text{iv}} = -1$, Eq. (A.11) becomes

$$\hat{\mathcal{F}}_{KL(n-1);ij}^{\rho} = \frac{\partial F_{KL(n-1)}}{\partial\rho_{ji}} c_i^{\dagger} c_j. \quad (\text{A.13})$$

Similarly, by treating all $\kappa_{i>j}$ and $\kappa_{i>j}^*$ as independent variables, the expressions

$$\hat{\mathcal{F}}_{KL(n-1);ij}^{\kappa} = \frac{1}{2} \frac{\partial F_{KL(n-1)}}{\partial\kappa_{ji}} c_i c_j \quad (\text{A.14})$$

and

$$\hat{\mathcal{F}}_{KL(n-1);ij}^{\kappa c} = \frac{1}{2} \frac{\partial F_{KL(n-1)}}{\partial\kappa_{ji}^*} c_j^{\dagger} c_i^{\dagger} \quad (\text{A.15})$$

give the summation of all different terms obtained by removing one contraction line in $F_{KL(n-1)}$ between c_i and c_j (c_i^{\dagger} and c_j^{\dagger}).

Since $\hat{\mathcal{F}}_{KL(n-1);ij}^{\rho}$ ($\hat{\mathcal{F}}_{KL(n-1);ij}^{\kappa}$, $\hat{\mathcal{F}}_{KL(n-1);ij}^{\kappa c}$) would be 0 if there is no contraction between c_i^{\dagger} and c_j (c_i and c_j , c_i^{\dagger} and c_j^{\dagger}) inside $\hat{\mathcal{F}}_{KL(n-1);ij}$, by summing up Eqs. (A.13) ~ (A.15) and summing over indexes i and j , one can get the sum of all terms that can be obtained by removing one contraction line in $F_{KL(n)}$:

$$\hat{\mathcal{F}}_{KL(n-1)} = \sum_{ij} \left(\hat{\mathcal{F}}_{KL(n-1);ij}^{\rho} + \hat{\mathcal{F}}_{KL(n-1);ij}^{\kappa} + \hat{\mathcal{F}}_{KL(n-1);ij}^{\kappa c} \right). \quad (\text{A.16})$$

Because any fully-but-two contracted term can always be obtained by removing one contraction line in a certain fully contracted term, by summing over all different $F_{KL(n-1)}$, one gets the sum of all fully-but-two contracted terms of $C_{KL(n-1)}$:

$$\begin{aligned} \hat{\mathcal{W}}_{KL(n-1)} &\equiv \sum_{\text{all F}} \hat{\mathcal{F}}_{KL(n-1)} \\ &= \sum_{ij} \left(\frac{\partial W_{KL(n-1)}}{\partial\rho_{ji}} c_i^{\dagger} c_j + \frac{1}{2} \frac{\partial W_{KL(n-1)}}{\partial\kappa_{ji}} c_i c_j + \frac{1}{2} \frac{\partial W_{KL(n-1)}}{\partial\kappa_{ji}^*} c_j^{\dagger} c_i^{\dagger} \right). \end{aligned} \quad (\text{A.17})$$

On the other hand, since two different fully contracted terms are still different after removing one contraction line in each, every fully-but-two contracted term only appears once in Eq. (A.17). In another word, Eq. (A.17) gives the sum of all different fully-but-two contracted terms of $C_{KL(n-1)}$.

One can then define an effective one-body operator

$$\begin{aligned} \hat{S}_{n-1} &\equiv \sum_{KL(n-1)} A_{KL(n-1)} \hat{\mathcal{W}}_{KL(n-1)} \\ &= \sum_{ij} \left(\mathcal{S}_{n-1;ij}^{\rho} c_i^{\dagger} c_j + \frac{1}{2} \mathcal{S}_{n-1;ij}^{\kappa} c_i c_j + \frac{1}{2} \mathcal{S}_{n-1;ij}^{\kappa c} c_j^{\dagger} c_i^{\dagger} \right), \quad (\text{A.18}) \\ \mathcal{S}_{n-1;ij}^{\rho} &\equiv \frac{\partial S_{n-1}}{\partial\rho_{ji}}, \quad \mathcal{S}_{n-1;ij}^{\kappa} \equiv \frac{\partial S_{n-1}}{\partial\kappa_{ji}}, \quad \mathcal{S}_{n-1;ij}^{\kappa c} \equiv \frac{\partial S_{n-1}}{\partial\kappa_{ji}^*}. \end{aligned}$$

In the above equation, \mathcal{S}_{n-1}^κ is a skew matrix:

$$\begin{aligned}\mathcal{S}_{n-1;ji}^\kappa &= \frac{\partial S_{n-1}}{\partial \kappa_{ij}} = -\frac{\partial S_{n-1}}{\partial \kappa_{ji}} \\ &= -\mathcal{S}_{n-1;ij}^\kappa.\end{aligned}\tag{A.19}$$

Similarly, $\mathcal{S}_{n-1}^{\kappa c}$ is also a skew matrix. With the help of this effective operator, the total contribution from the second type to S_n can be written as

$$\begin{aligned}S_{n;2} &= \sum_{ijkl} \left[\mathcal{S}_{n-1;ij}^\rho A_{n;kl} (\rho_{jk} \rho_{li}^{\text{iv}} - \kappa_{ki}^* \kappa_{jl}) \right. \\ &\quad + \frac{1}{2} \mathcal{S}_{n-1;ij}^\kappa A_{n;kl} (\rho_{jk} \kappa_{il} - \rho_{ik} \kappa_{jl}) \\ &\quad \left. + \frac{1}{2} \mathcal{S}_{n-1;ij}^{\kappa c} A_{n;kl} (\kappa_{ki}^* \rho_{lj}^{\text{iv}} - \kappa_{kj}^* \rho_{li}^{\text{iv}}) \right] \\ &= \text{Tr} [A_n (1 - \rho) \mathcal{S}_{n-1}^\rho \rho] - \text{Tr} [A_n^* \kappa^* \mathcal{S}_{n-1}^\rho \kappa] \\ &\quad - \text{Tr} [A_n \kappa \mathcal{S}_{n-1}^\kappa \rho] + \text{Tr} [A_n (1 - \rho) \mathcal{S}_{n-1}^{\kappa c} \kappa^*].\end{aligned}\tag{A.20}$$

By combining Eqs. (A.6) and (A.20), one gets

$$\begin{aligned}S_n &= \text{Tr} [A_n \rho] S_{n-1} + \text{Tr} [A_n (1 - \rho) \mathcal{S}_{n-1}^\rho \rho] - \text{Tr} [A_n^* \kappa^* \mathcal{S}_{n-1}^\rho \kappa], \\ &\quad - \text{Tr} [A_n \kappa \mathcal{S}_{n-1}^\kappa \rho] + \text{Tr} [A_n (1 - \rho) \mathcal{S}_{n-1}^{\kappa c} \kappa^*] \\ S_1 &= \text{Tr} [A_1 \rho].\end{aligned}\tag{A.21}$$

One should note that because all ρ_{ji} , $\kappa_{i>j}$ and $\kappa_{i>j}^*$ are treated as independent variables when calculating the partial derivatives of S_{n-1} , one cannot use the fact that the general density matrix is a projection operator to simplify the expression before the whole recursion is done.

The expression of S_n also holds for

$$S_n^{(r)} \equiv \frac{\langle \Phi | \mathcal{S}_n | \Phi(r) \rangle}{\langle \Phi | \Phi(r) \rangle},\tag{A.22}$$

which is the reduced kernel of \mathcal{S}_n between two different states $|\Phi\rangle$ and $|\Phi(r)\rangle$ with the same number parity. This is because in this situation, the fully contracted term $F_{KL(n)}$ would still be a product of contractions between two operators. However, the density and pairing tensor appearing in Eq. (A.21) should be replaced by the transition density and transition pairing tensor:

$$\rho \rightarrow \rho_r, \quad \kappa \rightarrow \kappa_r, \quad \kappa^* \rightarrow \kappa_r'^*.\tag{A.23}$$

This replacement leads to the relation (4.14).

Appendix B

Properties of kernels used in subsection 4.3.1

The simplex operator along $i = x, y, z$ axis is defined as

$$\hat{S}_i = \hat{\mathcal{P}} e^{-i\hat{J}_i\pi}, \quad (\text{B.1})$$

where $\hat{\mathcal{P}}$ is the parity operator and \hat{J}_i is the total angular momentum operator in the i -direction. If the mean-field state $|\Phi\rangle$ is invariant (up to a phase factor) under $\hat{S}_{i=x,y,z}$, it is easy to show that

$$\begin{aligned} \langle \hat{P}_i \rangle &\equiv \langle \Phi | \hat{P}_i | \Phi \rangle = 0, \quad i = x, y, z, \\ \langle \hat{P}_i \hat{P}_j \rangle &= 0, \quad \text{if } i \neq j, \end{aligned} \quad (\text{B.2})$$

where \hat{P}_i is the total momentum operator in the i -direction.

If the kernel \mathcal{N} can be calculated by using the GOA, there is:

$$\begin{aligned} \mathcal{N}(\mathbf{r}) &\equiv \langle e^{-i\hat{\mathbf{P}}_i \cdot \mathbf{r}} \rangle = \langle e^{-i(\hat{\mathbf{P}}_i \cdot \mathbf{n}_r)r} \rangle \approx \exp \left[-\frac{1}{2} \sum_{i,j=x,y,z} \langle \hat{P}_i \hat{P}_j \rangle r_i r_j \right] \\ &= \exp \left[-\frac{1}{2} \sum_{i=x,y,z} \langle \hat{P}_i^2 \rangle r_i^2 \right]. \end{aligned} \quad (\text{B.3})$$

In Eq. (B.3), the condition (B.2) is used. One thus obtains,

$$\begin{aligned} p_{2,j \neq i}(r_i) &= -\mathcal{N}(\mathbf{r})^{-1} \left. \frac{\partial^2 \mathcal{N}(\mathbf{r})}{\partial r_j^2} \right|_{r_k=0 \text{ for all } k \neq i} \approx \langle \hat{P}_j^2 \rangle - \left[r_j \langle \hat{P}_j^2 \rangle \right]_{r_j=0}^2 \\ &= \langle \hat{P}_j^2 \rangle = p_{2,j \neq i}(0). \end{aligned} \quad (\text{B.4})$$

This shows that $p_{2,j \neq i}(r_i)$ is a constant function of r_i in the frame of the GOA. Deviations from a constant value can thus appear only beyond GOA order and thus are ignored.

Bibliography

- [1] B. Carlsson, J. Dobaczewski, J. Toivanen, and P. Veselý, “Solution of self-consistent equations for the N3LO nuclear energy density functional in spherical symmetry. the program hosphe (v1.02),” *Computer Physics Communications*, vol. 181, no. 9, pp. 1641 – 1657, 2010.
- [2] N. Schunck, J. Dobaczewski, J. McDonnell, W. Satuła, J. Sheikh, A. Staszczak, M. Stoitsov, and P. Toivanen, “Solution of the skyrme-hartree-fock-bogolyubov equations in the cartesian deformed harmonic-oscillator basis.: (vii) hfodd (v2.49t): A new version of the program,” *Comput. Phys. Commun.*, vol. 183, no. 1, pp. 166 – 192, 2012.
- [3] M. Bender, P.-H. Heenen, and P.-G. Reinhard, “Self-consistent mean-field models for nuclear structure,” *Rev. Mod. Phys.*, vol. 75, pp. 121–180, Jan 2003.
- [4] T. Duguet, “The nuclear energy density functional formalism.” arxiv:1309.0440.
- [5] P. Navrátil, S. Quaglioni, I. Stetcu, and B. R. Barrett, “Recent developments in no-core shell-model calculations,” *J. Phys. G: Nucl. Part. Phys.*, vol. 36, no. 8, p. 083101, 2009.
- [6] G. Hagen, T. Papenbrock, D. J. Dean, and M. Hjorth-Jensen, “*Ab initio* coupled-cluster approach to nuclear structure with modern nucleon-nucleon interactions,” *Phys. Rev. C*, vol. 82, p. 034330, Sep 2010.
- [7] E. Epelbaum, H. Krebs, T. A. Lähde, D. Lee, and U.-G. Meißner, “Structure and rotations of the Hoyle state,” *Phys. Rev. Lett.*, vol. 109, p. 252501, Dec 2012.
- [8] G. Royer and C. Gautier, “Coefficients and terms of the liquid drop model and mass formula,” *Phys. Rev. C*, vol. 73, p. 067302, Jun 2006.
- [9] E. Caurier, G. Martínez-Pinedo, F. Nowacki, A. Poves, and A. P. Zuker, “The shell model as a unified view of nuclear structure,” *Rev. Mod. Phys.*, vol. 77, pp. 427–488, Jun 2005.
- [10] R. N. Schmid, E. Engel, and R. M. Dreizler, “Density functional approach to quantum hydrodynamics: Local exchange potential for nuclear structure calculations,” *Phys. Rev. C*, vol. 52, pp. 164–169, Jul 1995.
- [11] H. Nam, M. Stoitsov, W. Nazarewicz, A. Bulgac, G. Hagen, M. Kortelainen, P. Maris, J. C. Pei, K. J. Roche, N. Schunck, I. Thompson, J. P. Vary, and S. M. Wild, “UNEDF: Advanced scientific computing collaboration transforms the low-energy nuclear many-body problem,” *J. Phys: Conf. Ser.*, vol. 402, no. 1, p. 012033, 2012.
- [12] S. Bogner, A. Bulgac, J. Carlson, J. Engel, G. Fann, R. Furnstahl, S. Gandolfi, G. Hagen, M. Horoi, C. Johnson, M. Kortelainen, E. Lusk, P. Maris, H. Nam, P. Navratil, W. Nazarewicz, E. Ng, G. Nobre, E. Ormand, T. Papenbrock, J. Pei, S. Pieper, S. Quaglioni, K. Roche, J. Sarich, N. Schunck, M. Sosonkina, J. Terasaki, I. Thompson,

- J. Vary, and S. Wild, “Computational nuclear quantum many-body problem: The UNEDF project,” *Comput. Phys. Commun.*, vol. 184, no. 10, pp. 2235 – 2250, 2013.
- [13] W. Koch and M. C. Holthausen, *A Chemist’s Guide to Density Functional Theory, Second Edition*. New York: Wiley-VCH, 2001.
- [14] J. Dobaczewski, “Current developments in nuclear density functional methods,” *J. Phys: Conf. Ser.*, vol. 312, no. 9, p. 092002, 2011.
- [15] P. Ring and P. Schuck, *The Nuclear Many-Body Problem*. Berlin: Springer-Verlag Berlin Heidelberg, 1980.
- [16] J. Dobaczewski, “*Ab initio* derivation of model energy density functionals.” arxiv:1507.00697.
- [17] J. Rainwater, “Background for the spheroidal nuclear model proposal,” *Rev. Mod. Phys.*, vol. 48, pp. 385–391, Jul 1976.
- [18] J. Suhonen, *From Nucleons to Nucleus*. Berlin: Springer-Verlag Berlin Heidelberg, 2007.
- [19] F. Raimondi, *Higher-order Energy Density Functionals in Nuclear Self-consistent Theory*. PhD thesis, University of Jyväskylä, 2011.
- [20] K. Hebeler, T. Duguet, T. Lesinski, and A. Schwenk, “Non-empirical pairing energy functional in nuclear matter and finite nuclei,” *Phys. Rev. C*, vol. 80, p. 044321, Oct 2009.
- [21] M. Stoitsov, M. Kortelainen, S. K. Bogner, T. Duguet, R. J. Furnstahl, B. Gebremariam, and N. Schunck, “Microscopically based energy density functionals for nuclei using the density matrix expansion: Implementation and pre-optimization,” *Phys. Rev. C*, vol. 82, p. 054307, Nov 2010.
- [22] M. Kortelainen, T. Lesinski, J. Moré, W. Nazarewicz, J. Sarich, N. Schunck, M. V. Stoitsov, and S. Wild, “Nuclear energy density optimization,” *Phys. Rev. C*, vol. 82, p. 024313, Aug 2010.
- [23] B. G. Carlsson, J. Dobaczewski, and M. Kortelainen, “Local nuclear energy density functional at next-to-next-to-next-to-leading order,” *Phys. Rev. C*, vol. 78, p. 044326, Oct 2008.
- [24] F. Raimondi, B. G. Carlsson, and J. Dobaczewski, “Effective pseudopotential for energy density functionals with higher-order derivatives,” *Phys. Rev. C*, vol. 83, p. 054311, May 2011.
- [25] F. Raimondi, K. Bennaceur, and J. Dobaczewski, “Nonlocal energy density functionals for low-energy nuclear structure,” *J. Phys. G: Nucl. Part. Phys.*, vol. 41, no. 5, p. 055112, 2014.
- [26] P. Becker, D. Davesne, J. Meyer, A. Pastore, and J. Navarro, “Tools for incorporating a d-wave contribution in skyrme energy density functionals,” *J. Phys. G: Nucl. Part. Phys.*, vol. 42, no. 3, p. 034001, 2015.
- [27] J. A. Sheikh and P. Ring, “Symmetry-projected hartree-fock-bogoliubov equations,” *Nucl. Phys. A*, vol. 665, no. 1-2, pp. 71 – 91, 2000.
- [28] M. V. Stoitsov, J. Dobaczewski, R. Kirchner, W. Nazarewicz, and J. Terasaki, “Variation after particle-number projection for the hartree-fock-bogoliubov method with the skyrme energy density functional,” *Phys. Rev. C*, vol. 76, p. 014308, Jul 2007.

- [29] J. M. Yao, J. Meng, P. Ring, and D. P. Arteaga, “Three-dimensional angular momentum projection in relativistic mean-field theory,” *Phys. Rev. C*, vol. 79, p. 044312, Apr 2009.
- [30] P. Hohenberg and W. Kohn, “Inhomogeneous electron gas,” *Phys. Rev.*, vol. 136, pp. B864–B871, Nov 1964.
- [31] E. Engel and R. M. Dreizler, *Density Functional Theory: An Advanced Course*. Berlin: Springer-Verlag Berlin Heidelberg, 2011.
- [32] W. Kohn and L. J. Sham, “Self-consistent equations including exchange and correlation effects,” *Phys. Rev.*, vol. 140, pp. A1133–A1138, Nov 1965.
- [33] G. C. Wick, “The evaluation of the collision matrix,” *Phys. Rev.*, vol. 80, pp. 268–272, Oct 1950.
- [34] R. Machleidt and I. Slaus, “The nucleon-nucleon interaction,” *J. Phys. G: Nucl. Part. Phys.*, vol. 27, no. 5, p. R69, 2001.
- [35] T. Skyrme, “Cvii. the nuclear surface,” *Philos. Mag.*, vol. 1, no. 11, pp. 1043–1054, 1956.
- [36] T. Skyrme, “The effective nuclear potential,” *Nucl. Phys.*, vol. 9, no. 4, pp. 615 – 634, 1958-1959.
- [37] D. Vautherin, “Hartree-fock calculations with skyrme’s interaction. ii. axially deformed nuclei,” *Phys. Rev. C*, vol. 7, pp. 296–316, Jan 1973.
- [38] D. Vautherin and D. M. Brink, “Hartree-fock calculations with skyrme’s interaction. i. spherical nuclei,” *Phys. Rev. C*, vol. 5, pp. 626–647, Mar 1972.
- [39] J. Dechargé and D. Gogny, “Hartree-fock-bogolyubov calculations with the $d1$ effective interaction on spherical nuclei,” *Phys. Rev. C*, vol. 21, pp. 1568–1593, Apr 1980.
- [40] M. Dutra, O. Lourenço, J. S. Sá Martins, A. Delfino, J. R. Stone, and P. D. Stevenson, “Skyrme interaction and nuclear matter constraints,” *Phys. Rev. C*, vol. 85, p. 035201, Mar 2012.
- [41] E. Perlińska, S. G. Rohoziński, J. Dobaczewski, and W. Nazarewicz, “Local density approximation for proton-neutron pairing correlations: Formalism,” *Phys. Rev. C*, vol. 69, p. 014316, Jan 2004.
- [42] W. Satuła and R. A. Wyss, “Mean-field description of high-spin states,” *Rep. Prog. Phys.*, vol. 68, no. 1, p. 131, 2005.
- [43] J. Blaizot and G. Ripka, *Quantum Theory of Finite Systems*. Cambridge, MA, 1986.
- [44] J. Engel, “Intrinsic-density functionals,” *Phys. Rev. C*, vol. 75, p. 014306, Jan 2007.
- [45] J. Messud, M. Bender, and E. Suraud, “Density functional theory and kohn-sham scheme for self-bound systems,” *Phys. Rev. C*, vol. 80, p. 054314, Nov 2009.
- [46] J. Toivanen, J. Dobaczewski, M. Kortelainen, and K. Mizuyama, “Error analysis of nuclear mass fits,” *Phys. Rev. C*, vol. 78, p. 034306, Sep 2008.
- [47] M. Kortelainen, J. Erler, W. Nazarewicz, N. Birge, Y. Gao, and E. Olsen, “Neutron-skin uncertainties of skyrme energy density functionals,” *Phys. Rev. C*, vol. 88, p. 031305, Sep 2013.

- [48] J. Dobaczewski, W. Nazarewicz, and P.-G. Reinhard, “Error estimates of theoretical models: a guide,” *J. Phys. G: Nucl. Part. Phys.*, vol. 41, no. 7, p. 074001, 2014.
- [49] J. D. McDonnell, N. Schunck, D. Higdon, J. Sarich, S. M. Wild, and W. Nazarewicz, “Uncertainty quantification for nuclear density functional theory and information content of new measurements,” *Phys. Rev. Lett.*, vol. 114, p. 122501, Mar 2015.
- [50] D. G. Ireland and W. Nazarewicz, “Enhancing the interaction between nuclear experiment and theory through information and statistics,” *J. Phys. G: Nucl. Part. Phys.*, vol. 42, no. 3, 2015.
- [51] J. R. Donaldson and R. B. Schnabel, “Computational experience with confidence regions and confidence intervals for nonlinear least squares,” *Technometrics*, vol. 29, no. 1, pp. pp. 67–82, 1987.
- [52] L. F. Richardson and J. A. Gaunt, “The deferred approach to the limit. part i. single lattice. part ii. interpenetrating lattices,” *Phil. Trans. R. Soc. Lond. A*, vol. 226, no. 636-646, pp. 299–361, 1927.
- [53] J. Sadoudi, T. Duguet, J. Meyer, and M. Bender, “Skyrme functional from a three-body pseudopotential of second order in gradients: Formalism for central terms,” *Phys. Rev. C*, vol. 88, p. 064326, Dec 2013.
- [54] H. J. Lipkin, “Collective motion in many-particle systems: Part 1. the violation of conservation laws,” *Ann. of Phys.*, vol. 9, no. 2, pp. 272 – 291, 1960.
- [55] J. Dobaczewski, “Lipkin translational-symmetry restoration in the mean-field and energy-density-functional methods,” *J. Phys. G: Nucl. Part. Phys.*, vol. 36, no. 10, p. 105105, 2009.
- [56] X. B. Wang, J. Dobaczewski, M. Kortelainen, L. F. Yu, and M. V. Stoitsov, “Lipkin method of particle-number restoration to higher orders,” *Phys. Rev. C*, vol. 90, p. 014312, Jul 2014.
- [57] D. Thouless, “Stability conditions and nuclear rotations in the hartree-fock theory,” *Nucl. Phys.*, vol. 21, pp. 225 – 232, 1960.
- [58] N. Onishi and S. Yoshida, “Generator coordinate method applied to nuclei in the transition region,” *Nucl. Phys.*, vol. 80, no. 2, pp. 367 – 376, 1966.
- [59] G. F. Bertsch and L. M. Robledo, “Symmetry restoration in hartree-fock-bogoliubov based theories,” *Phys. Rev. Lett.*, vol. 108, p. 042505, Jan 2012.
- [60] F. Tondeur, S. Goriely, J. M. Pearson, and M. Onsi, “Towards a hartree-fock mass formula,” *Phys. Rev. C*, vol. 62, p. 024308, Jul 2000.
- [61] J. Erler, P. Klüpfel, and P.-G. Reinhard, “Self-consistent nuclear mean-field models: example skyrme-hartree-fock,” *J. Phys. G: Nucl. Part. Phys.*, vol. 38, no. 3, p. 033101, 2011.
- [62] Y. Nogami, “Improved superconductivity approximation for the pairing interaction in nuclei,” *Phys. Rev.*, vol. 134, pp. B313–B321, Apr 1964.